Evolution of October storm
Gravity wave detection
Lessons from Chernobyl
Closure of Binbrook

THE METEOROLOGICAL MAGAZINE

HER MAJESTY'S STATIONERY OFFICE

October 1988

Met.O.982 No. 1395 Vol. 117

METEOROLOGICAL OFFICE Met.O.982

THE METEOROLOGICAL MAGAZINE

No. 1395, October 1988, Vol. 117

551.515.11(420)

The synoptic–dynamical evolution of the storm of 15/16 October 1987

R.M. Morris

Assistant Director (Central Forecasting), Meteorological Office, Bracknell

Summary

The synoptic–dynamical evolution of the intense depression which caused widespread damage across southern England during the night of 15/16 October 1987 is described using Petterssen's development equation and the omega equation in conjunction with a series of composite charts displaying selected diagnostic parameters from the Meteorological Office operational numerical weather prediction models. The evolution of the storm is shown to be consistent with expectations using the equations and, in particular, the intensification of surface-pressure gradients on the southern flank of the depression during the evening of the 15th is ascribed to a combination of strong cold advection and strong advection of negative vorticity on the cold side upstream of the jet-stream core.

1. Introduction

The meteorological events leading up to, and those obtained in association with, the intense depression that caused widespread damage across southern England during the night of 15/16 October 1987 have been described in comprehensive detail in the April issue of the *Meteorological Magazine* (Meteorological Office 1988); this was based on the official report produced by the Meteorological Office (Meteorological Office 1987). The depression was most notable for the intense winds on its southern and western flanks which developed during the evening of the 15th over Biscay and Finisterre. The development of the storm, not unnaturally, requires some explanation and forecasters need to know whether there were any clues which, even with the benefit of hindsight, could be exploited to advantage in the future.

The Meteorological Office report on the storm includes a series of mean-sea-level pressure (PMSL) analyses redrawn after the event by experienced forecasters in the Central Forecasting Office (CFO) at Bracknell. These analyses were based upon a fully integrated assessment of the data available (i.e. including upper-air data and satellite imagery for example) and must represent the best set of analyses that could be obtained. The paucity of surface observations over the oceans during the development phase of the storm means that alternative analyses, in some details, cannot be entirely rejected. Nevertheless, for present purposes the official analyses are considered to be essentially correct.

Use will be made of the routine output of analyses from the Meteorological Office operational numerical weather prediction (NWP) models (Meteorological Office 1985) to monitor the evolution and development of the storm. NWP output has the great quality of internal consistency although phase errors in the location of systems can occur and careful subjective adjustments are required in such areas.

The period of study will be the 24 hours between 0000 GMT on 15 October and 0000 GMT on 16 October. The official report on the storm points out how sensitive the NWP forecasts were to variations in the analysis for 0000 GMT on the 15th. In particular, the differences between the operational fine-mesh model T+24-hour forecast and the same model forecast based upon an interpolated global model analysis (with later cut-off time for data) were startling, with the latter representing an excellent forecast by any standards. Nevertheless, the differences in the starting conditions for these model forecasts were not large and, realistically, no forecaster could be expected to spot these sort of deficiencies in the earlier analysis, even with access to satellite imagery, until the arrival of late data in the crucial areas. The aim of this paper is to demonstrate that forecasters can apply the fundamental dynamical principles that they are taught to use, in conjunction with the NWP output of diagnostic fields, to explain the broad-scale developments over the next 6 hours (exceptionally 12 hours) but not, realistically, any further ahead.

The information that the forecaster would seek to deduce on this occasion would be as follows:

(a) Trends in level of PMSL in any part of the area under consideration.
(b) Trends in direction of movement of the PMSL centres.
(c) Trends in speed of movement of the PMSL centres.

For these purposes it is considered that the operational NWP analyses should be adequate unless significant errors can be detected from the imagery and other sources, e.g. aircraft reports. Analyses at 0000, 1200, and 1800 on the 15th and 0000 GMT on the 16th will be used in conjunction with Meteosat imagery and, where inconsistencies with the latter are apparent, arguments will be advanced for careful modification to the NWP diagnostic fields with the consequences for short-period trends in the evolution of the weather system.

2. Basic principles

It is useful to briefly outline the two fundamental equations governing the diagnosis of vertical motion and the production of sea-level (i.e. PMSL) vorticity.

2.1 *The omega equation*

The vertical motion may be derived from the well known omega equation which in simplified form may be expressed thus:

$$\nabla^2\omega \approx \frac{\partial}{\partial p}\{\mathbf{V}.\nabla(\zeta+f)\} + \nabla^2(\mathbf{V}.\nabla T) \qquad \ldots \ldots \ldots \ldots \ldots (1)$$

where ω is the vertical motion in isobaric coordinates and the other symbols have their usual meaning. Large negative values of $\nabla^2\omega$ imply that ω is positive (i.e. descending air) and positive values of $\nabla^2\omega$ imply that ω is negative (i.e. ascending air). The omega equation is usually interpreted to infer that maximum values of ascending air in mid troposphere are associated with increasing (with height) positive advection of vorticity and also with maximum values of warm advection within the layer embracing the middle troposphere. Conversely, maximum values of descent are associated with upward-increasing negative advection of vorticity and maximum values of cold advection.

The practical usefulness of the omega equation lies in the fact that the two major forcing functions on the right-hand side of the equation are readily identifiable on standard working charts used by forecasters. Although current NWP models may not actually solve equation (1), the model vertical velocity fields can usually be interpreted from inspection of the omega equation (see, for example, Morris 1986). It is worth noting, however, that there are areas of the chart where the two terms on the right-hand side of equation (1) are large and opposite in sign, making interpretation difficult without access to the NWP vertical velocity fields. In such cases the distribution of vertical velocity may be partitioned vertically or is generally small. However, Hoskins *et al.* (1978) have derived an equation which combines the two terms into one and this can provide useful additional information in these cases.

2.2 *The equation for the PMSL vorticity*

The equation governing the production of PMSL vorticity is derived very lucidly by Petterssen (1956) and may be stated as follows:

$$\frac{\mathrm{d}Q_{1000}}{\mathrm{d}t} = -\underbrace{(\mathbf{V}_{500}\,.\nabla Q_{500} - \mathbf{V}_{1000}\,.\nabla Q_{1000})}_{\text{Ⓐ}} - \underbrace{\left(\omega\frac{\partial Q}{\partial p} - \frac{\partial \mathbf{V}}{\partial p}\times\nabla\omega.\mathbf{k} + Q_{500}\,\nabla.\mathbf{V}_{500}\right)}_{\text{Ⓑ}} - \underbrace{\frac{R}{f}\nabla^2\left(-\frac{g}{R}\mathbf{V}_{1000}\,.\nabla h_{\mathrm{TT}} + H + S\right)}_{\text{Ⓒ}} \quad \ldots \ldots \ldots \ldots (2)$$

where Q is the absolute vorticity and h_{TT} is the 1000–500 mb thickness; the subscripts refer to the standard pressure levels. The adiabatic heating term, H, and the static stability term, S, are given by

$$H = \ln\left(\frac{1000}{500}\right)\frac{1}{C_p}\frac{\mathrm{d}W}{\mathrm{d}t} \qquad S = \ln\left(\frac{1000}{500}\right)\overline{\omega(\Gamma_a - \Gamma)}$$

where Γ_a and Γ are the adiabatic and actual lapse rates in terms of pressure, and $\mathrm{d}W/\mathrm{d}t$ is the heat, other than latent heat, supplied to or removed from unit mass in unit time.

In order to interpret equation (2) it is useful to invoke the geostrophic assumption which implies a relationship between local changes of vorticity and contour height. For example, increases in cyclonic vorticity are equivalent to local maxima of falling contour height. The terms in equation (2) may be combined into three groups.

(a) Group A represents the difference in quasi-horizontal advection of vorticity between 1000 and 500 mb. Usually, and unless a strong circulation is present at sea level, the 500 mb term dominates this group. This implies, for example, that if, on synoptic charts, a fall of 500 mb contour height is advected across a region and is not matched by a comparable fall of PMSL heights through advection then, assuming the other terms in equation (2) are negligible, there must be a net fall of PMSL heights to balance the difference between the advection terms.

(b) Group B is usually fairly small; the vertical advection term transports vorticity from one level to another whilst the twisting term effects a rotation of thermal wind into the mean vorticity of the layer and vice versa. The divergence term can be very significant as a source of vorticity when the thermal advection tends to dominate the omega equation but in cases of strong coupling between upper-tropospheric vorticity advection and the lower troposphere, divergence at 500 mb probably has an insignificant role in equation (2).

(c) Group C is concerned entirely with the evolution of the thermal (1000–500 mb thickness) pattern under the influence of quasi-horizontal advection, diabatic heat transfer (through convection and radiation) and adiabatic cooling/heating associated with (dynamical) vertical motion. Latent heat is important in the last term. Equation (2) implies that, ignoring other terms, a local heating or cooling maximum will necessarily be associated with a fall or rise of PMSL vorticity respectively. (A simple exercise of gridding 1000 mb, thickness and 500 mb fields will demonstrate this fact.)

Equation (2) may be simplified by omitting the 1000 mb vorticity advection and the B group of terms to give

$$\frac{\mathrm{d}Q_{1000}}{\mathrm{d}t} = -\,\mathbf{V}_{500}\,.\nabla Q_{500} - \frac{R}{f}\nabla^2\left(-\frac{g}{R}\mathbf{V}_{1000}\,.\nabla h_{\mathrm{TT}} + H + S\right). \qquad \dots\ \dots\ \dots\ (3)$$

In principle, qualitatively at least, most if not all the terms in equation (3) can be identified on standard working charts used by forecasters.

2.3 *Application of the diagnostic equations to some idealized situations*

Fig. 1 illustrates some of the concepts described above which have a particular bearing on the development of the October 1987 storm. Fig. 1(a) depicts an idealized jet-stream core with 'entrance' and 'exit' regions. This contour-height field has exact mathematical form and it is easy to calculate the distribution of geostrophic vorticity. The pattern of vorticity advection is readily apparent and assuming this pattern dominates the upper troposphere with negligible advection in the lower troposphere then according to equation (1) there will be ascending air in mid troposphere beneath the cold exit and warm entrance regions and descending air beneath the cold entrance and warm exit regions. These relationships are confirmed by experience. It can also be seen (referring to equation (3)) that the jet stream propagates itself forward through the differential advection of vorticity at both exit and entrance regions. Neglecting the presence of significant thermal advection, the thermal field below the jet-stream level will, to a first approximation, advance closely in phase with the latter due to the adiabatic temperature changes associated with the vertical motion. Before considering how other terms in equation (2) cause phase adjustments between the contour and thermal fields to occur there is one other important aspect of the jet stream that needs to be pointed out. The entrance and exit regions have strong ageostrophic components of flow due to the acceleration and deceleration respectively of the air flowing through the pattern. Fig. 1(b) illustrates the relationship between the streamlines and contours in these regions of the jet stream. The whole of the upper-tropospheric air mass is descending in the confluence region and ascending in the diffluence region. The combined effects of Figs 1(a) and 1(b) are shown in schematic cross-section form in Fig. 1(c). It is not difficult to envisage how stratospheric air may be carried well into mid troposphere upwind and to the cold side of the jet-stream core.

The most common way in which sea-level vorticity develops through the mechanism of equation (3) is from the balance between upper-tropospheric vorticity advection and the static stability term (which controls the rate of heating and cooling in the presence of large-scale ascent or descent). Fig. 1(d) illustrates the development associated with an upper-tropospheric wave pattern in which the thermal pattern is initially in phase with the contour pattern (i.e. negligible thermal advection). It is assumed that the saturated air is characterized by an environmental lapse rate equal to the saturated adiabatic lapse rate and that the dry air is characterized by a lapse rate less than the dry adiabatic lapse rate. The contour wave pattern will progress in accordance with the quasi-horizontal advection of vorticity and there will be mid-tropospheric ascent ahead of the troughs and descent ahead of the ridges (equation (1), first term on the right-hand side). In the dry regions the static stability will be large and opposite in sign to the vorticity advection term (equation (2)) and this implies that the thermal pattern translates in close phase with the contour pattern. In the saturated regions the static stability term will be virtually zero implying (equation(3)) a net gain of vorticity in the PMSL field. This manifests itself as a retardation of the thermal pattern relative to the progression of the contour pattern, and a low-level circulation develops. Furthermore, it is readily apparent that if there is a source of diabatic heating, e.g. convection from a sea surface, in the area of ascending saturated air, the degree of cyclonic development will be much enhanced in the PMSL field.

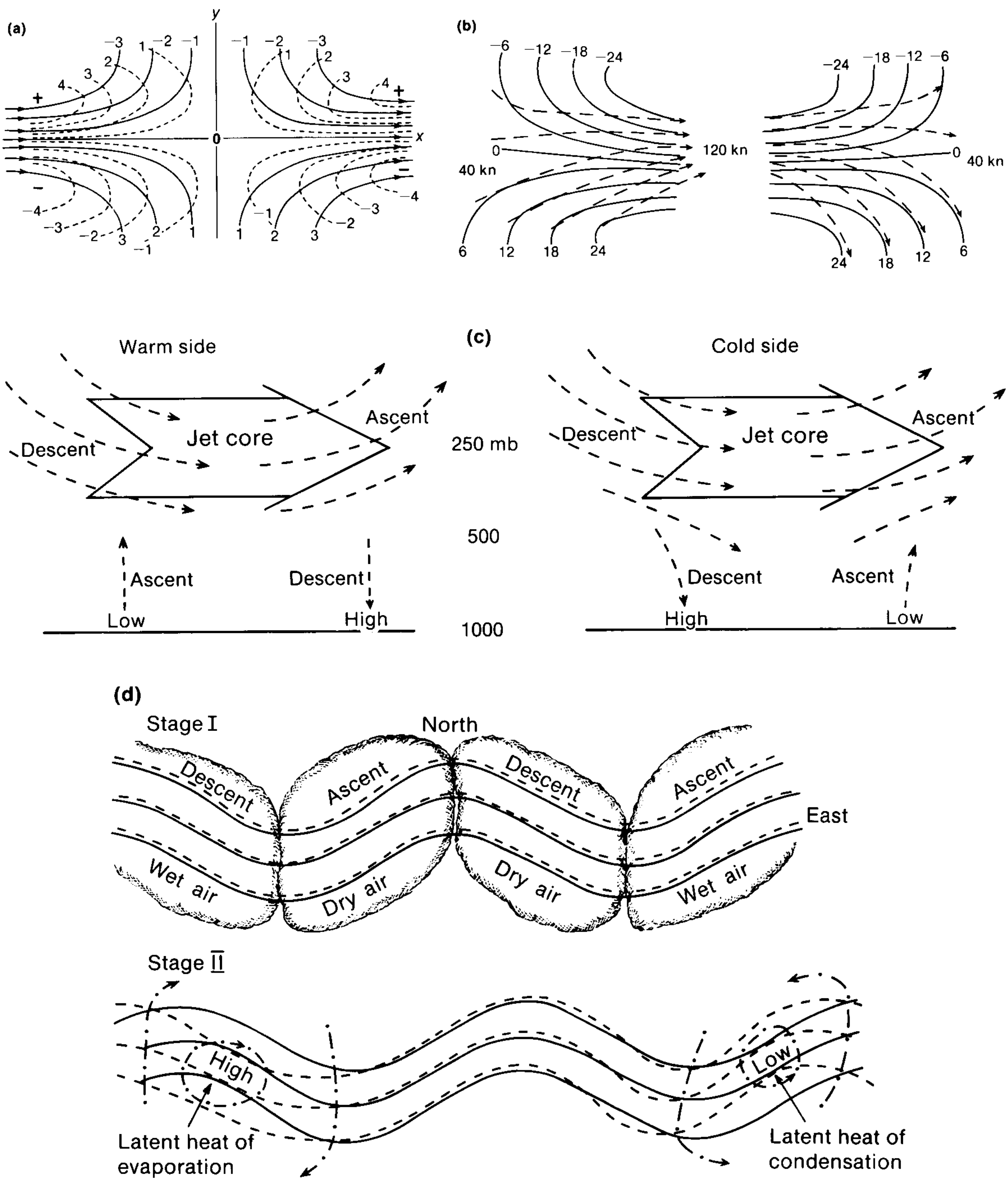

Figure 1. (a) Idealized geopotential height field at 500 mb (——) given by $h_{500} = \pm x \tan hy$ depicting jet-stream exit and entrance regions with associated geostrophic vorticity (– – –). (b) Streamlines (– – –) and contour field (——) at 250 mb indicating the ageostrophic motion. (c) Vertical profile of warm and cold sides of jet core showing ascent and descent regions. (d) Development of circulation in PMSL (•—•—) due to relative motion of 500 mb field (——) and 1000–500 mb thickness (– – –) through the influence of latent heat. The isopleths in (a) and (b) have arbitrary units.

3. Diagnostic charts

Before the advent of powerful computers and sophisticated NWP models, forecasting the evolution of synoptic-scale systems was based on quasi-subjective calculations of terms such as those contained in equations (1) and (3). Whilst it is indisputable that modern NWP model forecasts are much superior to quasi-subjective methods the fact is that NWP forecasts can occasionally be seriously in error for a number of reasons. One of the primary tasks facing forecasters must be to anticipate potential major errors in NWP guidance, effectively adding value to the guidance in the so-called man–machine mix process. However, in order to carry out this task forecasters must have a thorough perception of the relative importance of those terms in the equations that they can identify on any occasion; in other words they must monitor the synoptic evolution very closely.

Most of the output from the Meteorological Office NWP model is produced for specific forecasting tasks (e.g. forecasting wind, temperature, cloud and precipitation) but some output is used for diagnostic purposes. The diagnostic parameters may be combined and two composite charts in particular can be very useful:

(a) A composite consisting of the upper-tropospheric jet-stream core (speed and direction), PMSL isobars and a selection of total thickness isopleths superimposed upon the 850–500 mb mean vertical velocity and thermal advection analysis. This composite is designed to display cause and effect in the distribution of vertical velocity and contains explicitly two of the terms in equation (1). The jet-stream core is displayed to infer the sign and relative magnitude of the first term on the right-hand side in equation (1) and also, by induction, the first term on the right-hand side in equation (3). The distribution of thermal advection with respect to the thermal pattern demonstrates whether translation or amplification of the pattern is more likely. The distribution of vertical velocity with respect to the PMSL and thermal pattern allows a direct evaluation of the terms in equation (3) although the humidity and static stability distribution are still required.

(b) A composite consisting of PMSL isobars, and frontal boundaries deduced from the 850 mb wet-bulb potential analysis superimposed upon the model distribution of cloud (cloud is defined as relative humidity greater than or equal to 96% at any model level). As the model also parametrizes convection it is possible to display areas of (model) convective cloud for specific depths and tops reached. The usefulness of this composite is readily apparent. It shows the location and instantaneous movement of the boundary-layer air masses and their characteristics. Used with composite (a) it is possible to make direct evaluation of the sign and relative magnitude of the terms in equation (3).

It is particularly useful to compare these composites with satellite imagery thereby revealing possible deficiencies in the NWP model analyses. A sequence of these composite diagnostic analyses is used to illustrate the broad-scale development and evolution of the storm. Another composite chart consisting of the relevant satellite imagery with superimposed manually fine-tuned PMSL isobars and any other fields as appropriate, e.g. jet-stream analysis, will also be used. Specifically most attention will be focused upon the vorticity production within the centre of the low pressure complex as it transferred from north-east of the Azores to south-west England during 15 October 1987.

4. 0000 GMT on 15 October

At 0000 GMT (Fig. 2(a)) an elongated trough of low pressure was located west of Corunna (north-west Spain) extending over some 600 miles. The broad surface trough was closely related to a very strong baroclinic zone which was present in the lower and middle troposphere. The main surface centre was estimated to be at 43° N, 19° W with pronounced cold advection in the north and west quadrants, and warm advection in the south and east quadrants; thus the translation component due to thermal advection was strong.

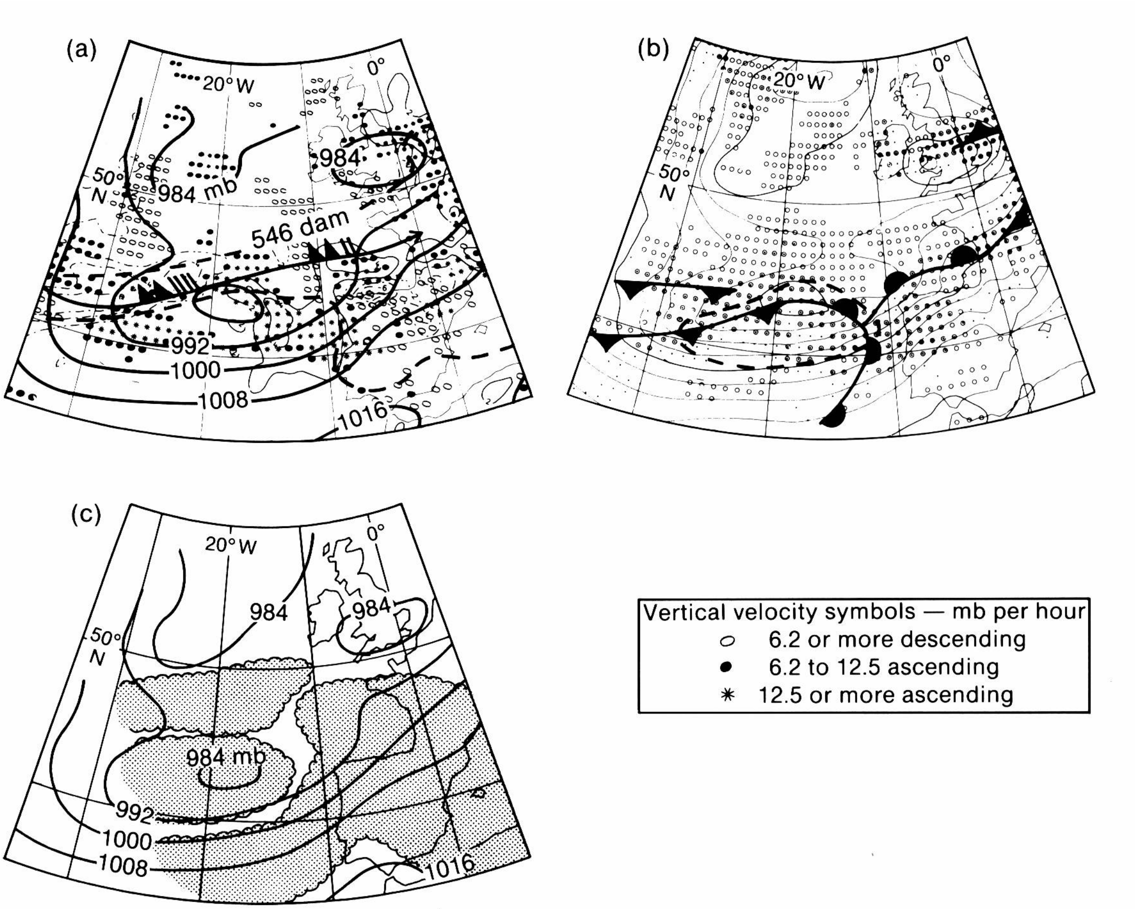

Figure 2. Charts for 0000 GMT on 15 October 1987: (a) composite fine-mesh model analysis showing jet-stream core (kn), 1000–500 mb thickness (– – –) and PMSL isobars (——) superimposed on the average (850–500 mb) fields of thermal advection (contours °C per 6 hours, solid lines warming, dashed lines cooling) and vertical velocity (see key), (b) composite fine-mesh model analyses of PMSL isobars (——), warm boundary of 850 mb wet-bulb potential temperature field ( ) and areas of deep convection (– – –) superimposed upon fields of medium (O) and low (●) cloud (cloud is defined as relative humidity $\geq$ 96% present at any model level — about four to choose from) and (c) manually fine-tuned PMSL isobars (——) and jet-stream core (kn) superimposed upon cloud areas obtained from satellite imagery ( ).

The baroclinic zone was associated with a very strong jet core in the upper troposphere and at this time the core speed maximum was located well to the west near 40° W. The diagnostic vertical motion field indicated ascending air across the whole of the broad surface trough with strong ascent over and just east of the main centre. Ascent extended well to the rear of the trough despite the presence of cold advection and this ascent was almost certainly associated with the positive vorticity advection on the cold side of the advancing jet stream. Indeed, the whole area of ascent west of the main surface low pressure centre must have been due to the positive vorticity advection whilst the strong ascent ahead of the surface centre was probably largely due to warm advection.

It is interesting to compare the diagnostic cloud analysis (Fig. 2(b)) with the corresponding Meteosat imagery (Fig. 2(c)) and to note how well the detail north-west of Corunna is represented by the model. The model convective cloud parametrization indicated some very deep instability (tops up to FL450) just on the warm side of the baroclinic zone within the broad surface trough.

The composite charts may be interpreted with equations (1) and (3) to make the following deductions about the development and evolution of the system. The surface circulation centred on 43° N, 19° W is associated with a thermal ridge, and strong ascent is evident on the northern and eastern flanks of this small system. Warm advection east of the surface centre and cold advection to the west beneath the jet core will translate the thermal ridge eastwards. The ascent will tend to cool the air adiabatically, but noting the presence of cloudiness and deep convective activity it is most likely that the latent heat supported by diabatic heat will tend to maintain the intensity of the thermal ridge despite the presence of ascent. Thus, strong PMSL vorticity production could be expected east of the surface centre due to positive contributions from all three thermal terms on the right-hand side of equation (3). This will manifest itself on the charts as translation plus some intensification of the thermal ridge. There is little indication of any significant change of PMSL vorticity within and just west of this centre. However, there is very strong ascent further west centred near 41° N, 27° W with a marked PMSL trough. This region of ascent is clearly associated with vorticity advection ahead of the upper trough; inspection of the terms in equation (3) suggests that strong PMSL vorticity production is likely within this PMSL trough due to the combined effects of vorticity advection aloft, and latent and diabatic release. This implies that as upper-contour heights fall above the PMSL trough a corresponding fall of total thickness due to adiabatic cooling will be mitigated by the local heating terms. This results in an increase in cyclonic circulation at the surface. Further north-west, beneath the cold side of the jet core, despite the dominance of vorticity advection over cold advection, the air appears drier and less unstable so that PMSL vorticity production will be a limited process. At the same time the combination of horizontal advection and adiabatic cooling will tend to cause a relatively rapid fall of total thickness towards the east and south-east.

5. 1200 GMT on 15 October

By 1200 GMT (Fig. 3(a)) the elongated surface trough was centred north-west of Corunna. The baroclinicity was at least as strong as analysed earlier but no distortion had occurred (nor indeed was expected with the symmetrical thermal advection about the associated thermal ridge, implying emphasis on translation). The surface trough had deepened significantly over a broad area consistent with the expectations (Fig. 3(d)). It seems reasonable to suppose that the centre located near 43° N, 19° W at 0000 GMT had moved to the Brest peninsula whilst the developing centre near 41° N, 27° W at 0000 GMT had moved to be north-west of Corunna. The jet core located above the surface trough was about as strong as earlier (maximum speeds about 140 kn) and the diagnostic vertical velocity revealed strong ascent being maintained across the whole surface trough. The strongest ascent was associated with strong warm advection but ascent was present over the surface centre and to the rear despite cold advection in the lower troposphere. Upper vorticity advection was almost certainly the cause of ascent in the middle troposphere to the north-west of Corunna. However, it was noteworthy that the region of strong descent beneath the main (i.e. strongest) jet core and associated strong cold advection had advanced considerably relative to the surface low pressure centre.

Comparison of the diagnostic cloud analysis (Fig. 3(b)) with Meteosat imagery (Fig. 3(c)) reveals how well the model appears to fit reality; however, there is one area of significant difference. Satellite imagery reveals a small coherent cloud system resembling a positive vorticity advection maximum (PVA) just west of 20° W, north of 40° N. The model has not only poorly represented this feature but also diagnoses descent in the region. Furthermore the model apparently failed to assimilate an aircraft report of 175 kn near 40° N, 25° W at 0905 GMT so it would appear that the model speeds are up to 30 kn light at the base and rear of the upper trough near 25° W. By inference there is probably ascent occurring in mid troposphere at 20–25° W on the cold side of the jet core and this would account for the presence of the PVA in the imagery.

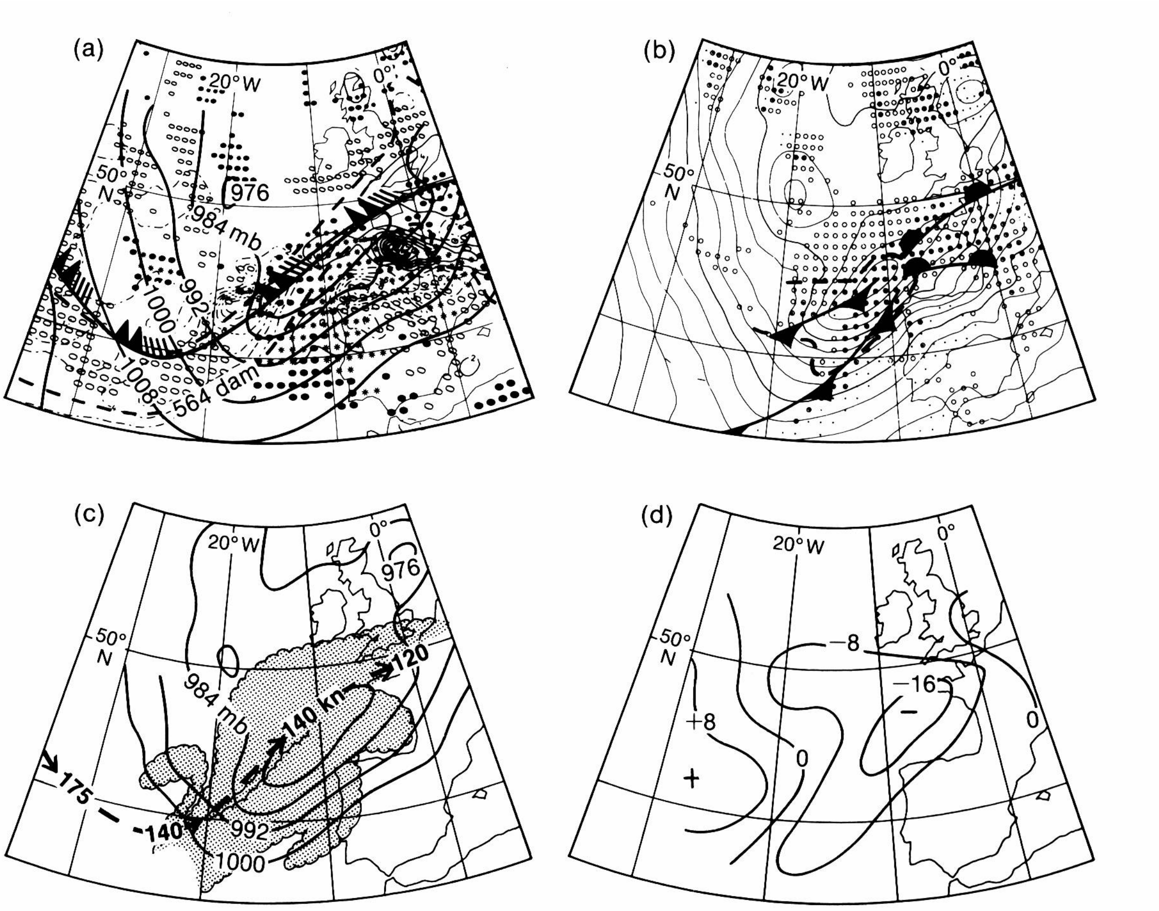

Figure 3. Charts for 1200 GMT on 15 October 1987: (a) to (c) as in Fig. 2 with (d) changes in PMSL (mb) during the previous 12 hours.

Despite the increase of circulation within the surface trough and strongly maintained ascent, 1000–500 mb total thickness values associated with the surface centre have remained virtually constant over the previous 12 hours. This indirectly reveals the combined effects of latent and diabatic heat transfer in the development process.

On the basis of the (modified) diagnostic analysis, further intensification of the surface pressure trough is to be expected. The main centre lies within a region of strong vorticity advection aloft, strong ascending air, a cloudy environment and associated convective activity; all factors combining to increase the PMSL cyclonic vorticity. At the same time the symmetry of thermal advection about the thermal ridge associated with the surface low pressure centre implies a strong element of translation being maintained. The magnitude of thermal advection had increased substantially over the past 12 hours especially in the regions flanking the main surface cyclonic centre and it was the cold advection that had increased the most.

Extrapolation of the above considerations leads to a possible conflict of developments. On the one hand the advancing west-north-west jet-stream core, with the associated PVA cloud cluster, may be expected to encroach even further upon the main surface trough causing more substantial cyclogenesis. On the other hand the region of strongest cold advection is now ahead of the west-north-west jet stream and would be expected to oppose the effects of the latter especially if cyclogenesis continues as expected due to vorticity advection aloft already in the region of the broad surface trough north-west of Corunna.

Some reference should be made to the appearance of an apparent dry 'slot' in the satellite imagery. This feature appears to be closely related to the jet core itself and its existence is probably linked to the dynamics of the air motion through the jet-core axis, as illustrated in Fig. 1, for example. In other words the dry slot represents a tracer which can identify the position of a strong jet-stream core.

6. 1800 GMT on 15 October

By 1800 GMT further intensification and deepening had occurred within the broad surface trough with the main cyclonic centre now located north of Corunna (Fig. 4(c)). Late data reveals that the operational numerical analysis (Figs 4(a) and 4(b)) has placed the cyclonic centre too far north-east towards the Brest peninsula. The necessary modification to the model diagnostics therefore includes a phase shift of the thermal ridge axis and corresponding shifts in the location of thermal advection maxima. The jet-core speed is about right though. The flow appears to be marginally anticyclonic at jet-stream level but it is not clear whether the diagnosed presence of ascent above the surface cyclonic centre is due most to vorticity advection at middle or at higher tropospheric levels. The magnitude of cold advection is still dominant, centred just north-west of Corunna. Significantly the diagnostic vertical velocity analysis reveals that descent has spread across the whole south-west quadrant of the surface cyclonic centre, indicating the increased dominance of cold advection. The phase adjustments to the model analysis described above should not affect the vertical velocity analysis relative to the system except that, with the likelihood of cold advection north-west of Corunna being even stronger, descent was probably correspondingly stronger.

The satellite imagery revealed significant changes during the 6 hours preceding 1800 GMT. The PVA cloud cluster lost definition and the main cloud mass to the north-west of the surface trough was showing signs of breaking up, probably due to strong descent, whilst a tongue of the lower cloud began to move east within the circulation of the intensifying cyclonic centre. The jet-stream analysis for 1800 GMT was consistent with the evolution in the satellite imagery; the jet core was clearly broken near 20° W and considerably weaker than hitherto in this region. The maximum wind speeds now appeared to be close to the position of the surface cyclonic centre. This evolution in the jet-stream structure over the 6 hours was highly significant and had dramatic consequential effects upon the evolution in the PMSL vorticity production. There is no direct evidence to prove that the 175 kn jet core at 1200 GMT did not subsequently propagate forward and encroach upon the surface trough, but the sequence of satellite imagery suggests that it did not do so. The associated PVA cloud cluster was clearly losing definition by 1500 GMT and there was the first sign of break up appearing in the main cloud mass at this time also.

Extrapolation of developments forward from this time needs careful assessment as follows:

(a) Although the areal extent of ascending air has been reduced considerably, ascent is still present above the surface cyclonic centre so that further deepening is to be expected. Whether the ascent is due to mid-tropospheric or upper-tropospheric vorticity advection, the direction of advection is towards the north-east so that the surface centre should be transferred north-east too.

(b) The cold advection through the baroclinic zone south-west of the cyclonic centre is very strong and considerably stronger than the warm advection in the zone north-east of the centre. More significant, however, is the change in sign of upper-vorticity advection; the south-west jet is now a separate feature and with the strongest winds apparently located above the PMSL centre; the region south-west of this centre and to the cold side of the jet core is an area of negative vorticity advection (see Fig. 1 for an example). Hence the thermal advection and vorticity advection terms are combining

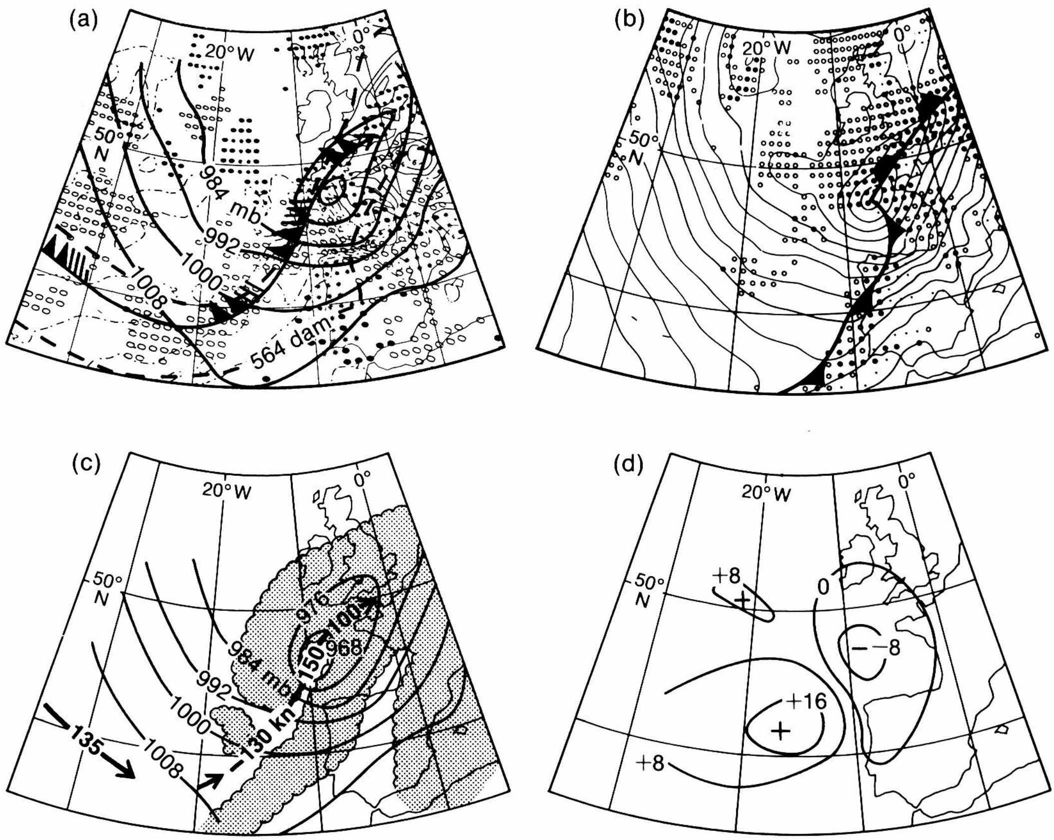

Figure 4. Charts for 1800 GMT on 15 October 1987: (a) to (c) as in Fig. 2 with (d) changes in PMSL (mb) during the previous 6 hours.

to produce strong descent and the production of anticyclonic vorticity in the PMSL field to the south-west of the surface centre. This manifests itself on the charts as a rise of upper-contour heights coupled to a fall of thickness values leading to a net strong rise of surface pressure. Thus, further deepening of the centre will lead to even stronger gradients in the south-west quadrant. Evidence that this evolution was already occurring at 1800 GMT is provided in Fig. 4(d) which illustrates the PMSL change over the preceding 6 hours.

7. 0000 GMT on 16 October

By 0000 GMT on the 16th the surface cyclonic centre had transferred north-east and deepened further, the deepening being more confined in areal extent than before, as expected. The surface gradients in the south-west quadrant had increased further, too, with very strong cold advection being maintained. Fig. 5(d) reveals in a spectacular fashion how the changing roles of the main dynamical forces created a substantial impact upon the PMSL. The 500 mb trough was almost vertically above the surface circulation and cyclonic vorticity was now present at 250 mb (not shown) directly above the surface system due presumably to deep upward penetration by the vertical transport of vorticity. The diagnostic vertical velocity (not shown) suggests that ascent was almost certainly confined to the north and descent confined to the south of the surface cyclonic centre so that further deepening was unlikely.

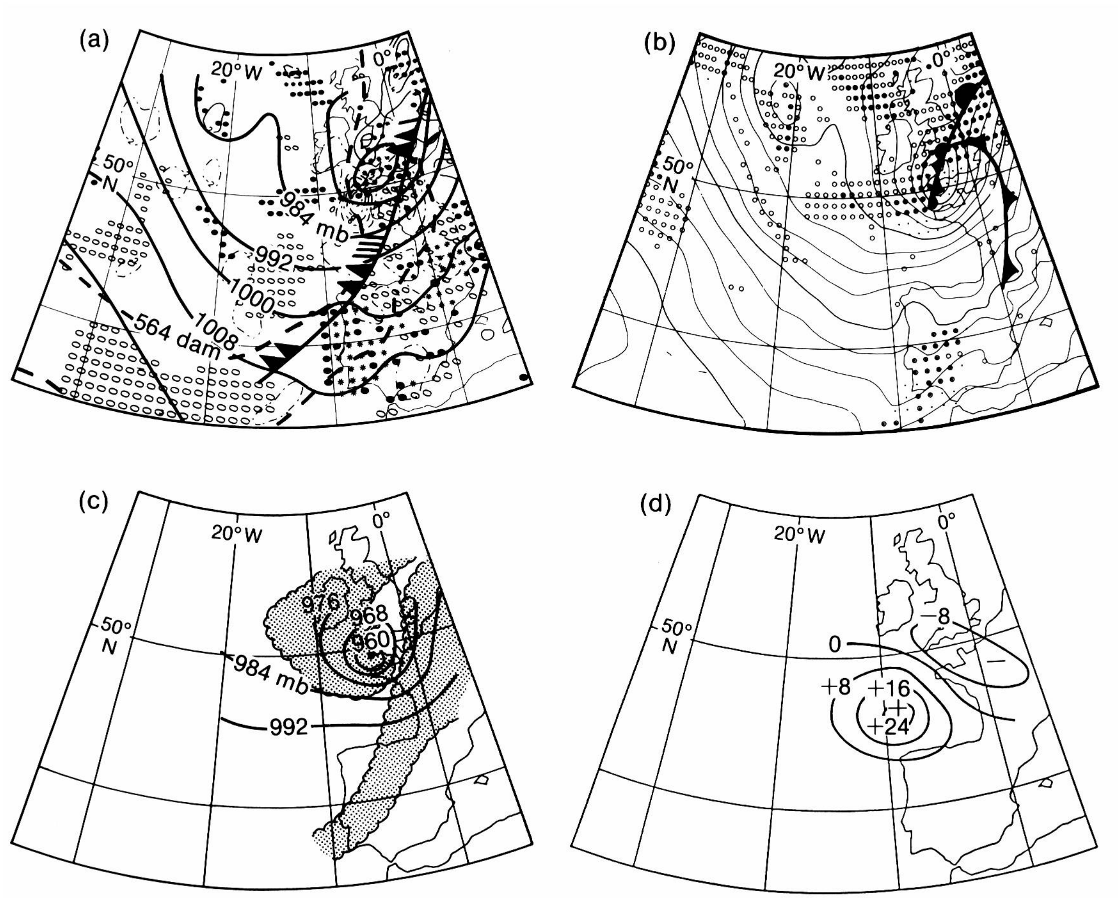

Figure 5. Charts for 0000 GMT on 16 October 1987: (a) to (c) as in Fig. 2 with (d) changes in PMSL (mb) during the previous 6 hours.

Significantly the baroclinicity has remained strong and undistorted so that the thermal advection fields, which were still symmetric about the thermal ridge axis, would combine directly with the vorticity advection fields to maintain rapid north-east movement beyond this time.

8. Concluding remarks

It has been demonstrated that the evolution of the intense depression which affected southern England during the night of 15/16 October 1987 can be explained, at least in qualitative terms, by reference to basic equations and using composite diagnostic analyses derived from the NWP model. This itself is of some comfort because if composite diagnostic analyses of the sort described in this paper can be made operationally available quick enough to be useful there is a good chance that the forecaster can make important decisions more quickly and more confidently than would otherwise be possible. In the case of the storm described in this paper, it was not until the 1800 GMT analysis was fully diagnosed that the exceptionally strong surface pressure gradients to the rear of the system could be anticipated with any real conviction. Under present operational conditions such deductions would be made between 2100 and 2200 GMT. In future, improvements in data processing should bring this period forward by an hour at least.

Finally it is interesting to compare the evolution of the maximum wind pattern as portrayed in the composite sequences in Figs 2 to 5 with the sequence of 250 mb wind forecasts from one of the rerun fine-mesh forecasts based upon the optimum analysis at 0000 GMT on the 15th. Two such fine-mesh forecasts are described in the official storm report (Meteorological Office 1987) and both produced excellent PMSL forecasts for successive stages in the development phases during the 15th. Fig. 6 is taken from the storm report. The most significant difference is at 1200 GMT in the position of the jet-stream maximum (compare Fig. 3(a) with T+12 in Fig. 6). If, as is suggested here, the PVA cloud cluster (as shown in Fig. 3(c)) identified the jet-stream cold exit position at 1200 GMT then the T+12 forecast in Fig. 6 is, strictly, incorrect in some detail. However, the T+18 forecast is reasonably consistent with Fig. 4(c) which could be interpreted as also supporting the suggestion here that the upstream jet-core

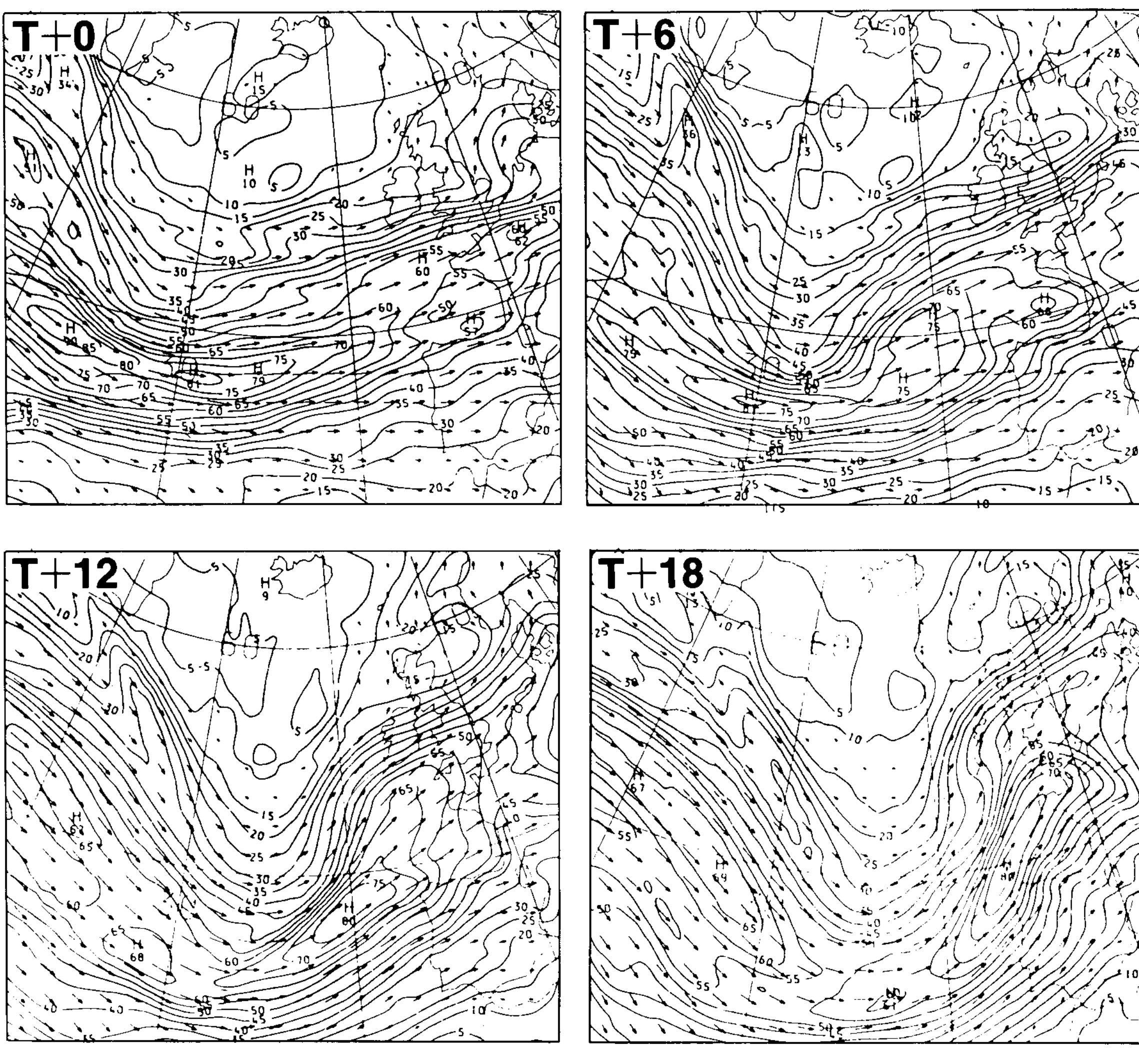

Figure 6. 250 mb winds (m s^{-1}) from a rerun fine-mesh forecast based upon the optimum analysis at 0000 GMT on 15 October 1987. Length of arrows is proportional to wind speed.

PVA cloud cluster became an irrelevance to the further development of the storm. Diabatic heating from the warm sea on the cold side of the baroclinic zone could possibly explain the weakening of the upstream jet maximum which probably occurred between 0900 and 1500 GMT with dramatic consequences for the dynamical evolution of the storm during the subsequent 9 hours.

References

Hoskins, B.J., Draghici, I. and Davies, H.C.	1978	A new look at the ω-equation. *Q J R Meteorol Soc*, **104**, 31–38.
Meteorological Office	1985	Operational numerical forecasting. *Meteorol Mag*, **114**, 221–291.
	1987	The storm of 15/16 October 1987. Bracknell, Meteorological Office.
	1988	Report on the storm of 15/16 October 1987. *Meteorol Mag*, **117**, 97–140.
Morris, R.M.	1986	The Spanish plume — testing the forecaster's nerve. *Meteorol Mag*, **115**, 349–357.
Petterssen. S.	1956	Weather analysis and forecasting Volume I. New York, McGraw-Hill.

551.558.21:551.508.822:551.524.77(412)

A large amplitude gravity wave detected by radiosonde*

G.J. Shutts and M. Kitchen

Meteorological Office, Bracknell

P.H. Hoare

Meteorological Office, Shanwell

Summary

The routine operational radiosonde launched from Shanwell in Scotland at 2318 GMT on 12 December 1986 recorded very large variations in temperature in the lower stratosphere. These were accompanied by strong vertical shear in the horizontal wind and large variations in the rate of ascent of the balloon. There are indications that these disturbances were due to quasi-stationary gravity waves.

1. Introduction

The UK RS3 radiosonde system provides highly reproducible temperature measurements combined with a very fast time constant of response. Similarly, the operational Cossor radar is capable of resolving fine structure in the horizontal wind profiles on a vertical scale of a few hundred metres and amplitude of the order of 1 metre per second. Much of the detail in the operational radiosonde sounding is discarded when the TEMP messages are composed but is clearly of value in research projects.

Whilst it is widely recognized that the breaking of gravity waves exerts a powerful influence on the middle atmosphere circulation, only recently has the influence of inertia-gravity wave motion on tropospheric flow been considered seriously by numerical modellers. Unfortunately, the sort of information required by the modeller — large-scale, area-averaged vertical momentum fluxes — is not available. The case-study presented here deals with an extreme gravity wave event over mountains of modest stature and provides some insight into the kind of information about gravity waves that can be obtained from radiosonde data.

---

* An abridged version of a paper by Shutts, Kitchen and Hoare (1988) which appeared in the *Quarterly Journal of the Royal Meteorological Society*.

2. The observations

The routine radiosonde launched from Shanwell at 2318 GMT on 12 December 1986 recorded very large amplitude excursions in temperature in the lower stratosphere which were identified as being exceptional by the staff at the radiosonde station. The detailed profiles of temperature and wind derived from the RS3 radiosonde system fine-structure archive are given in Fig. 1. To put the ascent in context, the balloon trajectory is given in Fig. 2 and the synoptic situation is illustrated in Fig. 3.

Fig. 1 shows that between 15.5 and 22 km the radiosonde encountered strong vertical gradients in temperature and wind. In particular, at the stable layer around 15.7 km, the measured temperature increased by 9.9 °C for a change in computed geopotential height of only 134 m. This very stable layer was followed by an essentially isentropic layer about 2 km deep (see inset profile of potential temperature in Fig. 1(a)), and over this layer the total fall in temperature was 15.9 °C. Above 18 km another very stable layer was encountered, although not as pronounced as that at 15.7 km, followed by a deep layer with an average lapse rate of approximately 5 °C km^{-1} but interrupted by three small inversions. The radiosonde balloon burst at an altitude of 24.1 km.

These large temperature variations were accompanied by strong vertical shear in the horizontal wind speed profile. The bases of the two stable layers identified above were both associated with local maxima in the wind speed profile (see Fig. 1(b)) and the isentropic layer was a region of much lighter wind. The transitions between the intense stable layers and the isentropic layer were marked by substantial changes in wind speed and direction.

The rate of ascent of the balloon computed from the change in radiosonde geopotential with time between adjacent data points in the fine-structure archive is plotted in Fig. 1(d). The mean rate of ascent of the balloon through the stratosphere was about 6 m s^{-1} but superimposed on this mean value were variations of $\pm$6 m s^{-1}. In the two stable layers bounding the isentropic layer the ascent rate was observed to fall to close to zero, whereas in the isentropic layer itself the ascent rate was enhanced by over 5 m s^{-1}. The close agreement between these rates of ascent and those computed from the data from the Cossor wind-finding radar prove that the variations in the rate of ascent were real.

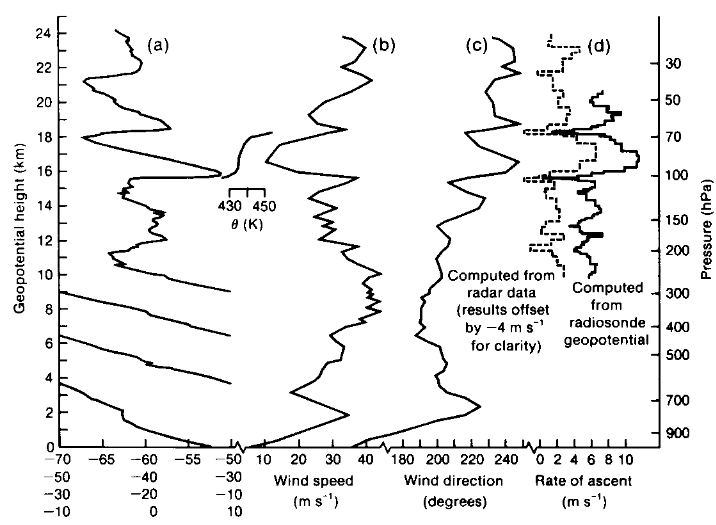

Figure 1. Profiles from the radiosonde launched at Shanwell at 2318 GMT on 12 December 1986 showing (a) temperature and potential temperature (θ), (b) wind speed, (c) wind direction and (d) rate of ascent computed from radar data and radiosonde geopotential.

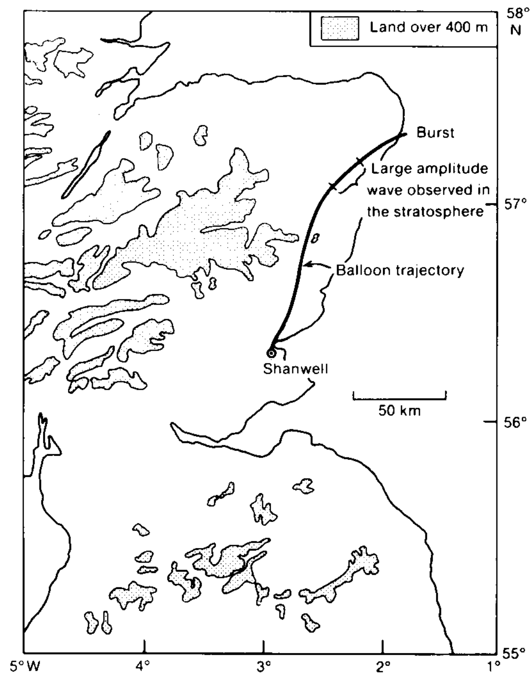

Figure 2. Balloon trajectory of the Shanwell ascent at 2318 GMT on 12 December 1986.

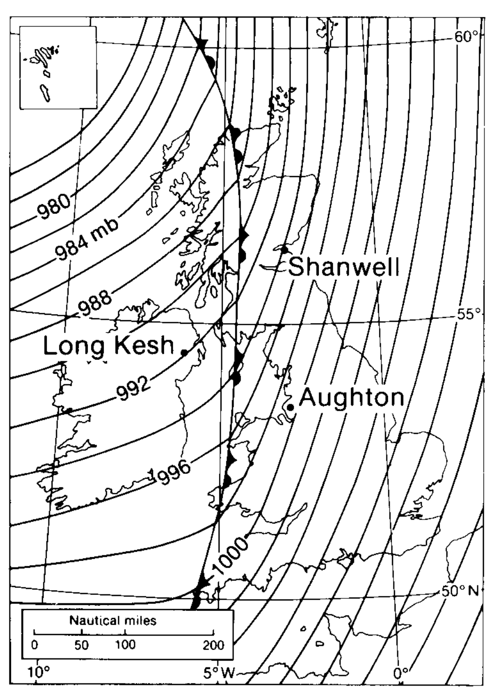

Figure 3. Synoptic situation at 0000 GMT on 13 December 1986 plus location of stations mentioned in the text.

Ascents from Shanwell at 1117 GMT on 12 December and 1118 GMT on 13 December show that the features in the stratospheric temperature and wind profiles shown in Fig. 1 were ephemeral. The geographical distribution of the fluctuations was investigated by examining the ascents from Aughton and Long Kesh. They also showed strong variations in temperature (10 °C over 2 km at Long Kesh) in the lower stratosphere but there were no obviously sympathetic fluctuations in wind speed and ascent rate.

3. Theoretical interpretation

A simple model of finite-amplitude gravity wave motion can be used to interpret the balloon observations.

For two-dimensional incompressible flow with constant wind speed and static stability it is possible to derive an expression for the streamlines of finite-amplitude gravity waves. From this the horizontal and vertical wind components can be derived.

A sinusoidal stationary wave solution may be used to model the ascent of an idealized radiosonde balloon through a uniform airstream with a gravity wave. It will be assumed that the balloon travels with the velocity of the ambient flow plus an upward component equal to the rate of ascent of the balloon in an atmosphere at rest. This allows the trajectory of the idealized balloon to be computed exactly and provides some simple mathematical expressions for the values of potential temperature which would be observed by the radiosonde (details are given in Shutts *et al.* 1988*).

Fig. 4 shows the profile of potential temperature measured vertically through a gravity wave and that seen by a balloon passing through the wave (various parameters derived from the Shanwell ascent have been used). The balloon perceives a markedly different 'vertical wavelength' as it samples phase variations in its horizontal as well as vertical motion fields. Where the downward motion of the air becomes comparable with the balloon's ascent, a marked fictitious inversion appears. For example, when the downward speed in the gravity wave exactly equals the 'still air' rate of ascent of the balloon, the balloon is no longer ascending yet it will still record a change in potential temperature as it moves horizontally through the stationary wave field.

Some of the features illustrated in Fig. 4 also appear in Fig. 1. For example, the marked inversion near 15.7 km in Fig. 1(a) is related to the decreased rate of ascent of the balloon to close to zero; even so a highly stable layer is still implied. In addition to shallow stable layers, there are layers which are nearly isentropic where the balloon travels upward at almost twice its 'still-air' ascent rate.

Determination of the vertical wavelength of the gravity wave is complicated by the slantwise ascent of the balloon: the apparent wavelength in Fig. 1(a) will be a mixture of horizontal and vertical phase variations, as in Fig. 4. However, the simple wave model provides strong evidence that the disturbance is a quasi-stationary gravity wave with horizontal and vertical wavelengths of about 16 and 6 km respectively, although there is some uncertainty about the actual phase speed.

The negative correlation between the fluctuations in the horizontal wind and vertical motion in the lower stratosphere (see Fig. 1) indicates that the gravity wave was accompanied by a downward momentum flux. Dr S. Mobbs and Ms J. Rees from the Mathematics Department of the University of Leeds have computed the momentum flux from the fine-structure data. They found that between 16 and 17 km, the downward momentum flux is approximately 3.3 N m^{-2} which is over ten times larger than the surface frictional drag expected in non-mountainous regions. Such a substantial flux of momentum implies a powerful influence on the lower stratospheric flow — albeit over a limited region.

* Shutts, G.J., Kitchen, M. and Hoare, P.H.; A large amplitude gravity wave in the lower stratosphere detected by radiosonde. *Q J R Meteorol Soc*, **114**, 1988, 579–594.

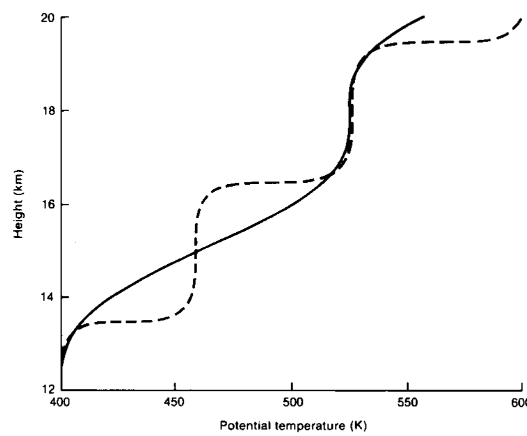

Figure 4. Potential temperature variation in a sinusoidal gravity wave measured vertically (solid line) and following an idealized radiosonde balloon (dashed line).

4. Conclusions

This study of the Shanwell ascent at 2318 GMT on 12 December 1986 demonstrates the potential of operational radiosonde soundings for analysing the structure of stationary, orographic gravity waves. Using a long period of routine radiosonde observations, it may be possible to build up a picture of the frequency and geographical distribution of gravity wave breaking in the lower stratosphere. This might be sufficient to permit the verification of gravity wave parametrization schemes now being used in operational weather prediction models.

551.577.7(41-4):551.556.4

Lessons from the dispersion and deposition of debris from Chernobyl

F.B. Smith

Meteorological Office, Bracknell

Summary

Radioactivity escaped from the wrecked reactor at Chernobyl for 10 days and spread over most of Europe. Part of the debris crossed Britain a week after it was emitted. Heavy thunderstorms and a northward-moving cold front washed out much of the radioactive iodine and caesium, especially on to the upland areas of North Wales, northern England, south-west Scotland, and Ulster. Several lessons have been learnt, including information on the dry and wet removal rates. These lessons are discussed in this paper.

1. The accident

The release of radioactive debris into the atmosphere from Reactor 4 at the nuclear power plant at Chernobyl in the Ukraine was the most serious in the history of the civil nuclear industry.

The disaster started in the early morning of 26 April 1986 during a rather special experiment. The aim was to test the safety of the reactor should two breakdowns occur simultaneously: firstly should the steam from the reactor suddenly fail to reach the great turbine generators and secondly should the supply of electricity from the national grid to the turbines be cut off. The question then was: would the mechanical inertia of rotation of the turbines be sufficient to generate enough electricity to keep such vital components as the pumps working within the reactor for up to 50 seconds before stand-by diesel generators could be started and take over the necessary supply?

In fulfilment of this experiment the power of the reactor was brought to well below 20% of normal power in spite of the fact that the particular design of the reactor at Chernobyl was known to become potentially unstable at such low levels. At 0123 local time this instability was realized and the reactor accelerated from a small fraction of full power to 100 times full power in just 4 seconds, causing an explosive generation of steam and the rupturing of pipes and protective shielding. The core was now exposed to the air and rapid chemical reactions resulted causing a second explosion. The reactor building was destroyed and burning graphite and core debris were spewed out over the site and into the atmosphere.

The loss of radioactive material to the atmosphere persisted for nearly 10 days in spite of valiant efforts to seal the reactor with about 5000 tonnes of material dropped from helicopters. Roughly 2×10^{18} becquerels of activity were released into the air during this period, about a third of which went out in the first few hours. (A becquerel (Bq) represents one atomic disintegration per second.) Debris released in this early period was very hot and rose 1 or 2 kilometres into the atmosphere. Later emissions were much cooler and travelled largely within the boundary layer over long distances except when advected upwards at fronts or in large convective clouds.

2. The spread of debris over Europe

At the time of the explosion a ridge of high pressure was centred over north-west USSR (see Fig. 1(a)). The wind circulation associated with this ridge carried the upper part of the plume away towards the Baltic Sea and Scandinavia. Nearer the ground, the nocturnal clear skies had resulted in the development of a 500 m deep surface-based inversion. This inversion, whilst not preventing the sedimentation of the larger particles in the airborne debris, helped to insulate the local population from

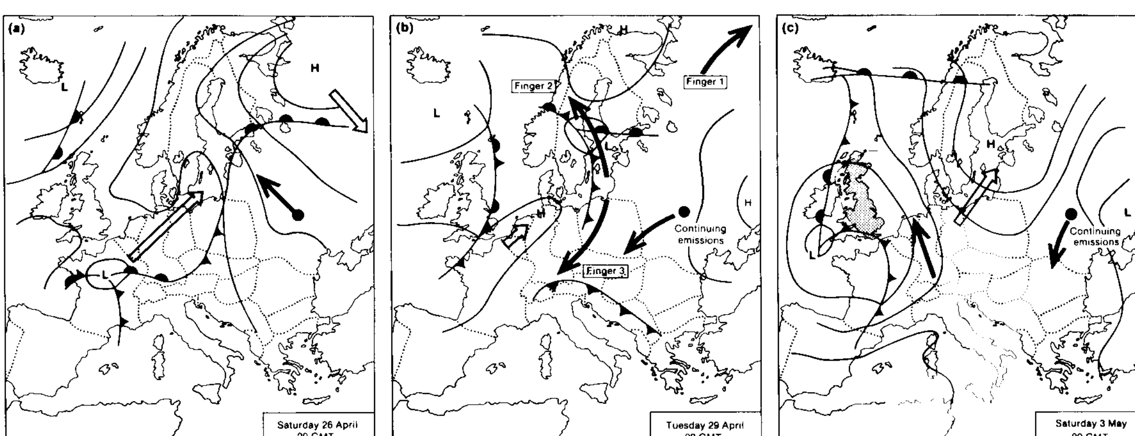

Figure 1. Schematic maps for (a) 0000 GMT on 26 April 1986, (b) 0000 GMT on 29 April 1986 and (c) 0000 GMT on 3 May 1986 showing how synoptic developments influenced the spread of radioactive debris from Chernobyl (●) in the days following the accident; ⇨ indicates movement of synoptic features, ⟶ movement of part of the Chernobyl cloud, and stippled area position of radioactive cloud over the United Kingdom.

the downward diffusion of the inhalable small particles which could have caused a great deal of damage within peoples' lungs.

Once the plume reached Scandinavia, it split into three 'fingers' (see Fig. 1(b)). One moved away to the east across northern parts of the USSR into Japan and China. A second finger, caused by a jet ahead of the cold front of an active depression, crossed central Norway and the Norwegian Sea and moved towards North America. Heavy rain which affected this finger on 28 April resulted in very large depositions of activity in central Scandinavia which contaminated the lichens and mosses, the main diet of the Lapp reindeer. A third finger moved south-westwards in response to a transient ridge of high pressure which followed the depression across north-west Europe. This finger moved across central Europe and the Alpine areas into France and then turned northwards, entering the United Kingdom in the early hours of Friday, 2 May (see Fig. 1(c)).

3. Passage over the United Kingdom

The passage of the debris over Britain makes an interesting story which can only be summarized here. A fuller description is given in Smith and Clark (n.d.). Beautiful warm spring weather on Friday, 2 May experienced over much of Britain was soon replaced by wet and stormy conditions on the Saturday and Sunday as a depression to the south-west of Cornwall deepened and an associated cold front moved into the country. Additionally, the warm air moving in from France ahead of the front became increasingly unstable and thunderstorms developed over the south-east of England in the early hours of Saturday; these moved fitfully north-westwards and caught up the main body of the cloud of debris over North Wales and northern England. The storms drew great quantities of contaminated low-level air into their systems causing considerable rainfall and heavy depositions, particularly in Snowdonia, the Skipton area of Yorkshire, Cumbria, the Isle of Man, Ulster and south-west Scotland. Parts of the radioactive cloud were drawn off to the west across Ireland by the circulation of the depression, but most of the debris continued to move northwards, the tail of the cloud eventually leaving the northernmost parts of Scotland by the end of Sunday. However, small traces of activity were detected later in the subsequent week as parts of the debris drawn off by the depression recrossed the country. Some of these features can be seen in Fig. 2.

4. Deposition of hazardous nuclides

The cloud of debris contained a host of different radio-nuclides originating from the reactor. From a health point of view the most important of these were iodine-131, a short-lived isotope which gets into milk and then into human thyroids, caesium-134 with a half-life of about 2 years, and caesium-137 with a half-life of 30 years. The caesium isotopes can accumulate in the human body and, like the iodine-131, can cause cancer. Nevertheless, the risk of this is very small indeed and, except in the most heavily contaminated areas around Chernobyl itself, increases in cancer incidence within the population are likely to prove undetectable. The main pathway for these isotopes into the body is through foodstuffs and not by direct inhalation. Consequently the activity has to be deposited first on the ground. This deposition arises not just from the 'cleansing' action of rain, a process generally termed 'wet deposition', but also from dry deposition — the combined effect of sedimentation of larger particles under gravity, impaction of particulates and aerosols on leaves etc., and absorption of reactive gases by the soil and vegetation.

Dry deposition depends on the product of the concentration, C, of the material close to the surface and a so-called 'deposition velocity', v_d:

$$\text{Dry deposition} = v_d C.$$

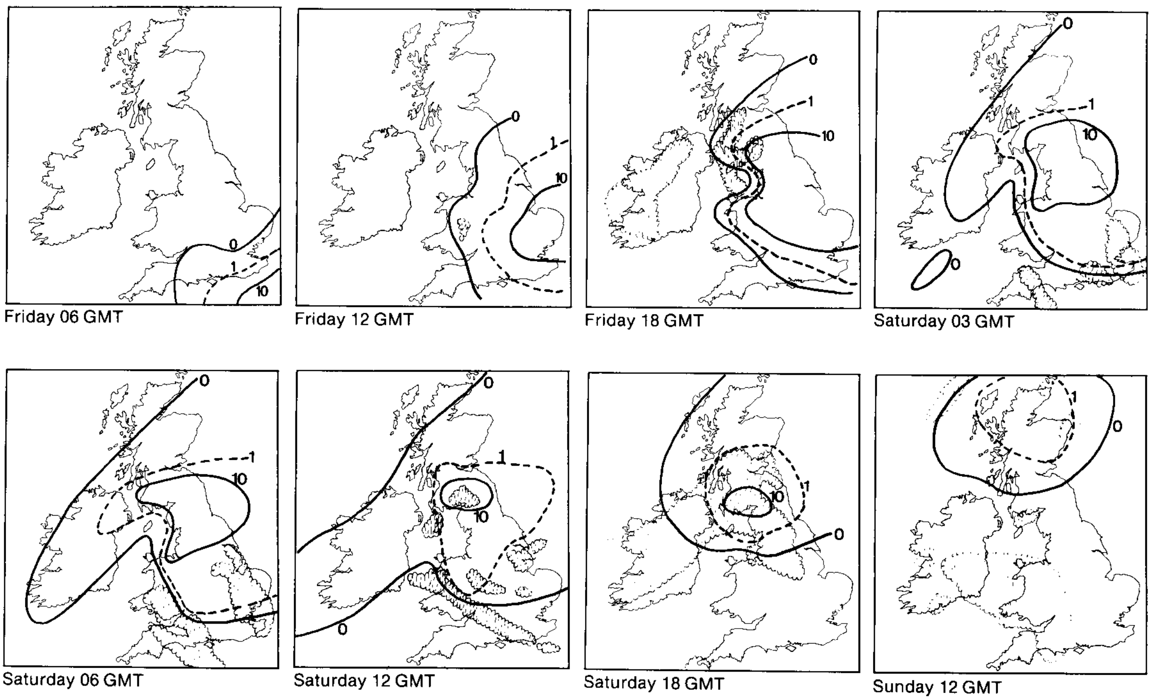

Figure 2. Position of radioactive cloud at various times as shown. Hatched areas indicate where some rainfall was reported and hence where significant wet deposition of radioactivity may have been occurring. Contours are in becquerels per cubic metre.

By comparison with wet deposition, dry deposition is rather slow — just 1 mm of rain can remove more material than can dry deposition operating over 24 hours. However, dry deposition is an almost continuous process whereas wet deposition is usually very intermittent. Consequently, in the deposition of acidifying species (in the acid rain problem) dry deposition is more important than wet deposition except in a few very wet areas of Europe like the Norwegian mountains.

In the Chernobyl debris, iodine-131 was partly gaseous in form and partly particulate. The gaseous component dry-deposited some eight times more rapidly than the particulate component. This can be inferred from the relative concentrations and depositions of both particulate caesium-137 and iodine in areas where no rain occurred (on the assumption that particulate iodine deposited as efficiently as the caesium).

The wet removal is assumed to follow the simplified expression:

$$\text{Wet deposition} = wCR$$

where C is the average concentration in the air during the rain, R is the rainfall expressed in millimetres and w is an empirically determined coefficient. Units of concentration are becquerels per cubic metre and units of deposition are becquerels per square metre. Based on measured depositions and air concentrations the following values of v_d and w have been inferred:

Iodine-131, gaseous: $v_d = 0.4\ \text{cm s}^{-1}$, $w = 490$,
particulate: $v_d = 0.05\ \text{cm s}^{-1}$, $w = 650$.
Caesium-137, particulate: $v_d = 0.05\ \text{cm s}^{-1}$, $w = 650$.

5. Rainfall over the United Kingdom

In the first few days and weeks following the passage of the Chernobyl debris over the United Kingdom the only rainfall data available in sufficient detail were from the weather radar output. Although the radar coverage at that time only covered England, Wales and the most southern parts of Scotland the picture provided was extremely useful and sufficiently accurate to pin-point the areas most likely to have been significantly contaminated by deposition. By July 1986 enough surface rain-gauge data had become available for a reasonable rainfall map for the whole of the United Kingdom to be drawn up, although it was not until late September that a complete quality-controlled map could be prepared. Fig. 3 shows this final rainfall picture. The values represent the rainfall which actually intercepted the radioactive cloud. Two points are of particular interest: firstly the convective storms resulted in narrow but very elongated 'footprints' of rainfall and secondly it is clear that the strength of the storms responded in a quite dramatic way to the nature of the terrain over which they were passing. Level uniform countryside tended to weaken the storms whereas large cities (e.g. London), mountains, and stretches of sea like the Solway Firth, rapidly strengthened them.

6. Total depositions

Fig. 4 gives the estimated deposition for caesium-137 over the United Kingdom using the deposition parameters given above in conjunction with the rainfall data implicit in Fig. 3 and the assessed concentrations of caesium-137 in the air. The levels of deposition vary enormously over the country and the highest values reflect the areas of heaviest rainfall. The maximum estimated deposition is in excess of 30 000 Bq m^{-2} near Whithorn in Dumfries and Galloway. These depositions and the corresponding ones for iodine-131 can be integrated over the whole of the United Kingdom and compared with the estimated emissions from Chernobyl:

Iodine-131: Total deposition on the United Kingdom = 2×10^{15} Bq,
Deposition as a fraction of total emission = 0.7%,
Deposition as a fraction of first day's emission = 2%.
Caesium-137: Total deposition on the United Kingdom = 3×10^{14} Bq,
Deposition as a fraction of total emission = 0.8%,
Deposition as a fraction of first day's emission = 3%.

The depositions are compared with the emissions on the first day of the accident because trajectory analyses indicate that the debris that crossed the United Kingdom was emitted in a roughly 2-hour slot in the late morning of 26 April. It is interesting that a higher percentage of the caesium emission than of the iodine emission on that day was deposited on the United Kingdom; this can only be because the iodine, being partly gaseous, had lost more *en route* by dry deposition before reaching this country.

Caesium-134 is believed to have behaved in a very similar manner to caesium-137, and in fact was used to distinguish deposited caesium-137 arising from Chernobyl from that previously in the ground which had its origins in the weapons tests of the 1950s and 1960s. During the passage of the Chernobyl debris the concentration of caesium-134 was typically just over half that of the caesium-137. Consequently the total caesium-134 deposition on the United Kingdom is inferred to be about 1.5×10^{14} Bq.

7. Agricultural effects

The consequences for agriculture in the United Kingdom were only of real significance in sheep farming. In all other aspects of agriculture the levels of activity were well below the emergency reference levels set by the Government (except for some game birds and freshwater fish in limited parts of

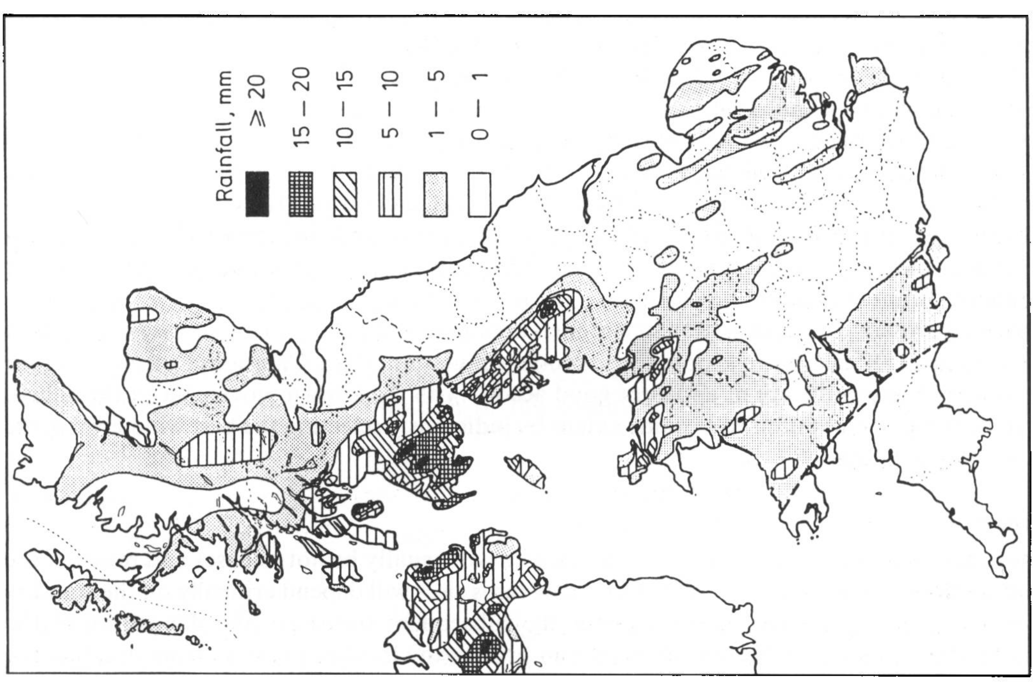

Figure 3. Rainfall, determined from over 4000 rain-gauge measurements, which intercepted the radioactive cloud. Rain which did not fall when the cloud was overhead is excluded. Dashed line indicates the south-western border of the debris.

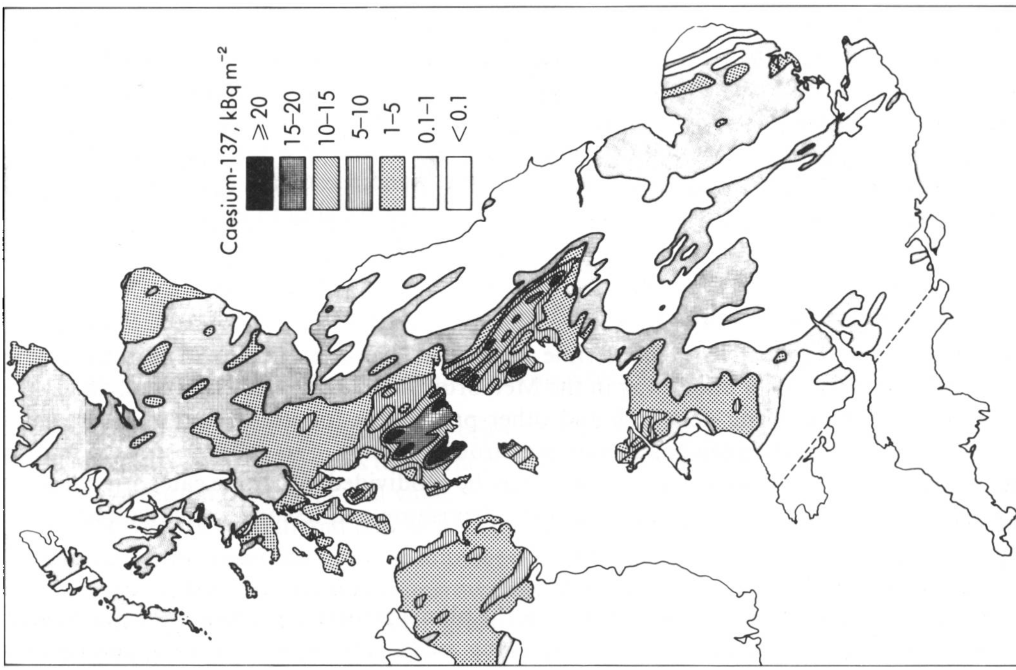

Figure 4. Empirically derived total depositions of caesium-137. Dashed line indicates the south-western border of the debris.

south-west Scotland). Unfortunately many upland sheep-farming areas were affected by relatively heavy depositions of caesium-137, and this led to restrictions on the movement and slaughter of sheep on farms where levels in the sheep in excess of 1000 Bq kg^{-1} have been recorded. To make matters worse, levels have changed only very slowly on some of these farms in contrast to the more rapid decline observed in many lowland areas. The important element appears to be the nature of the soil. Soils rich in clay minerals rapidly lock in the free caesium so that it becomes unavailable to the vegetation. Poor acidic soils typical of many upland areas are unable to do this and the caesium cycles through the uppermost humic layers of the soil and the vegetation so that its availability to grazing sheep falls off only very slowly.

8. Summary of the lessons of Chernobyl

A new perspective has been gained from the terrible accident at Chernobyl. This will be invaluable in the preparation of new models now under way in the Meteorological Office and elsewhere, and in the design and operation of monitoring networks and other procedures for use should another major accident ever occur. This perspective can be summarized through a listing of so-called 'lessons'. Limiting these to those with some meteorological interest, they may be subdivided into three categories: lessons regarding transport in the atmosphere, lessons regarding deposition and lessons for agriculture.

8.1 *Transport and dispersion*

(a) Synoptic-scale deformation: Close to the source, the plume probably behaved very much like a conventional plume from a factory chimney, growing under the action of three-dimensional turbulence in a quasi-conical manner. When the width of the plume exceeded 100 to 200 kilometres, the synoptic variations of velocity became dominant and the plume then grew through deformation as described by Gifford (1987).

(b) Wind shear in the vertical: Changes of wind speed and direction with height through the plume were principal factors in diluting the concentration within the plume, especially when deformation became dominant. Dilution occurs when shear is coupled with vertical mixing, either concurrently or successively through a diurnal cycle.

(c) Correction of trajectories using radiological data: Although it appears that most trajectory analyses carried out on the Chernobyl release have been reasonably successful in predicting the spread of the debris over Europe, it is almost certain that individual trajectories starting from Chernobyl at the same time differed significantly at long range and the apparent overall success simply reflects the very variable meteorological situation during the whole release. In other circumstances, differences might be more obvious. Radiological reports of activity would then be invaluable in optimizing the information that models are capable of giving. Fig. 5 shows the output of the Meteorological Office's basic Monte Carlo model simulation of the Chernobyl accident at four different times; these results are in apparent good accord with the known movement of the debris. This agreement has been optimized to some extent by judiciously selecting the best wind level in the light of radiological data.

8.2 *Deposition*

(a) Atmospheric stability at the source: Large releases will usually be hot releases and much of the airborne debris will rise away from the surface. How far is rises will depend critically on the stability of the air, and this will have consequences for the subsequent transport and deposition of the material. As seen earlier, a stable surface layer can protect the local population from much of the small inhalable particles and radioactive gases.

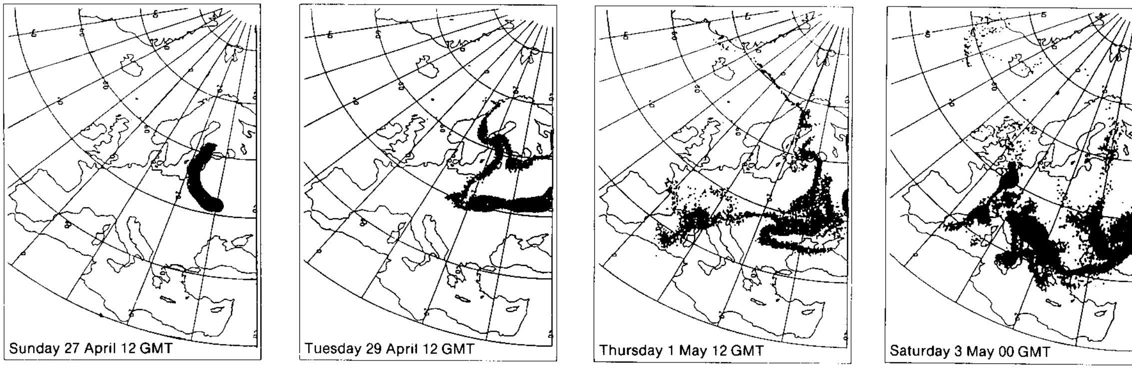

Figure 5. Simulation of the movement of debris from Chernobyl using a two-dimensional Monte Carlo model.

(b) Deposition rates for differing species: Washout rates and dry deposition velocities will differ significantly from one species to another, and these need to be well known in advance of any accident if model output is to be of real value.

(c) Convective rainfall and deposition shows banded structure: As evident in Figs 3 and 4, rainfall and deposition resulting from the thunderstorms during the passage of the Chernobyl debris over the United Kingdom were banded in narrow elongated 'footprints'. Interpolation between measurements of caesium-137 (for example) on grass or in soil should therefore be carried out with strong along-wind weighting and not with simple circular weighting.

8.3 *Agriculture*

(a) The importance of wet deposition: The Chernobyl accident has emphasized how much more efficient wet deposition is compared with dry deposition whenever rain occurs. Agriculturists wishing to monitor levels of deposition rapidly should therefore concentrate initially on areas where significant rain intercepted the debris. Quick help for this can be obtained from operational weather radar as long as the debris' movement is roughly known from models or from monitors in the field.

(b) Retention on vegetation: In areas where little or no rain occurred most of the deposition was through dry deposition and a high percentage was retained on the vegetation available to grazing animals. In areas of significant rain the total deposition may have been much higher but retention on the vegetation appeared to have been only some 10–25% of the deposited particulates, and very small indeed for the gases. This effect was very evident in the levels of iodine-131 in milk: levels in comparatively dry areas were not dramatically smaller than in wet areas for these reasons (Clark and Smith 1988).

(c) The influence of soil type on long-term effects: As seen from the aftermath of Chernobyl, soil type can critically influence the duration of the continued contamination of foodstuffs and grazing animals.

References

Clark, M.J. and Smith, F.B. 1988 Wet and dry deposition of Chernobyl releases. *Nature*, **332**, 245–249.

Gifford, F.A. 1987 The time-scale of atmospheric diffusion considered in relation to the universal diffusion function, f_1. *Atmos Environ*, **21**, 1315–1320.

Smith, F.B. and Clark, M.J. (n.d.) The transport and deposition of airborne debris from the Chernobyl nuclear power plant accident, with special emphasis on the consequences to the United Kingdom. *Sci Pap, Meteorol Off*, No. 42. (To be published.)

551.501.9:358.4(425)

Closure of Meteorological Office at Royal Air Force Binbrook

J.G. Leslie
Meteorological Office, Royal Air Force Binbrook

The decision by the Royal Air Force to close their Strike Command airfield at Binbrook, Lincolnshire will terminate a Meteorological Office association with the locality dating back to the early years of the last war.

Meteorological Office staff, in uniform, were first drafted into Binbrook in 1940. Initially they supported Fairey Battle squadrons, then Wellingtons, and later, 460 Squadron of the Royal Australian Air Force flying Lancasters.

After the war the airfield remained active, but with observers and forecasters moving back into mufti. The first jet aircraft to arrive were Canberra bombers in 1951, which generated a need for meteorological information up to the low stratosphere on a regular basis. In 1960 staff were dispersed as the airfield came under Fighter Command, and an extensive reconstruction and runway lengthening programme was undertaken. Javelin squadrons were the first to arrive on reopening in 1962, but it was in 1965 that the aircraft arrived that were to have the longest and best known connection with Binbrook — the Lightnings. These supersonic air defence fighters of Numbers 5 and 11 Squadrons have remained until the present day, often on 24-hour alert against possible intruders from eastern airspace. New standards of vigilance in observing and short-term forecasting were demanded by the weather sensitivity and short endurance of these aircraft. However, judging by the lack of weather-related accidents in the last twenty-odd years, one may claim that the requirements have been well met.

It has not always been a comfortable life at Binbrook. In the fifties and sixties the office was accommodated in prefabricated huts which shook and whistled in the wind. Telephone calls were made from acoustic booths in which one bellowed against the roar of nearby jet engines. In 1968 peace and

quiet arrived in the form of a first-floor sound-proofed office, with a magnificent panoramic view over the airfield and surrounding areas — a great improvement.

Being sited on a ridge, atop the Lincolnshire Wolds, Binbrook has been famous for its exposed position. Nicknamed 'Windy Hill' by generations of airmen, as they were forced to adopt an almost permanent list from leaning into gusts around the hangars, it has generally lived up to its name. (A frequent, but discrete, source of amusement for hardened resident staff has been to watch occasional visitors as their eyes water and ears turn blue!) Records support the popular conception, with calculated mean wind speeds of 13 to 14 knots in the winter months, falling only a little to a mean of 9 to 10 knots in the summer. The maximum speed recorded was 50 knots with gusts to 78 knots in the winter gale of January 1976.

The hilly site has at least prevented any great extremes of temperature, with a maximum of 32.1 °C and a minimum of −12.6 °C being recorded in July 1969 and February 1986 respectively.

In winter any substantial fall of snow could be guaranteed to block access to the camp, as drifting from the large Lincolnshire fields filled in around the roadside hedges. The most notable occurrence of this was in February 1979 when a period of snow followed by frequent snow showers, together with north-easterly winds gusting to 45 knots, caused drifts 1 metre deep on the open airfield and in excess of 5 metres on some nearby roads. The snow was far too deep to be ploughed and eventually had to be dug out. The station was cut off for 5 days, with the staff 'trapped' on duty making round-the-clock observations and living from tins! Seldom has a winter passed without a similar occurrence, albeit not so severe.

For all that, though, the area is generally very pleasant, with a rather quiet, rural way of life and the complete absence of urban stresses. Many of the staff have, on a fortuitous posting, chosen to settle down and raise their families in this peaceful corner, contentment overcoming their ambitions.

In addition to the upheaval for the present staff, it is certain that Binbrook's closure will also create a significant gap in the observing network. With the lack of detailed information from the coastal strip, easterly winds have always brought problems for eastern England; Binbrook has acted as an outpost, warning of low cloud and sea fog for stations further inland. Will automatic stations fill the need?

Award

The Buchan Prize of the Royal Meteorological Society was received jointly by Dr G.J. Shutts (Forecasting Research Branch of the Meteorological Office) and Dr T.N. Palmer (at ECMWF on special leave from the Meteorological Office). It was presented for Dr Shutts' work on the forcing of blocking anticyclones by transient eddies, for Dr Palmer's work (with Dr S. Zhaobo) on the effect of North Atlantic sea surface temperature anomalies on the general circulation, and for their collaborative work (with R. Swinbank) on the parametrization of gravity-wave drag in numerical weather prediction models.

Dr Shutts' paper on blocking showed how synoptic systems approaching a split jet-stream pattern became elongated in the meridional direction and, under certain conditions, give up their energy so as to reinforce the blocking pattern.

Dr Palmer and Dr Zhaobo used a general circulation model to show that sea surface temperature anomalies in the north-west Atlantic give a statistically significant downstream response. The resulting 500 mb height anomalies were supported by an observation study using two independent 30-year periods of data.

The work of Dr Shutts, Dr Palmer and Mr Swinbank on gravity-wave drag gave convincing evidence, both theoretical and observational, that small gravity waves should exert a powerful drag force in the lower troposphere and lower stratosphere. In a study using a general circulation model, they demonstrated that a known systematic westerly bias in the wind direction could be removed by parametrizing the drag force due to breaking gravity waves. Similar parametrization schemes are now being used in most operational weather forecasting models.

Notes and news

Retirement of Dr W.T. Roach

Dr W.T. Roach, Assistant Director (Meteorological Research Flight) retired from the Meteorological Office on 5 August. He first joined the Office in 1953 as a Temporary Scientific Officer at Kew Observatory following a period in the Royal Electrical and Mechanical Engineers doing military service and at Imperial College where he obtained a BSc in physics and an MSc in meteorology. A year later he returned to Imperial College where he obtained a PhD on solar and infra-red emission spectra through the atmospheric window. This research brought him into early contact with the water vapour continuum, a topic which is of continuing interest to his group at the Meteorological Research Flight.

When, as a Senior Scientific Officer, Dr Roach returned to the Office in 1958 his first posting was in fact to the Meteorological Research Flight at Farnborough where he worked for Bob Murgatroyd on ozone and humidity measurements from aircraft. This was a time when the tropopause fold was coming into fashion and some of his studies were concerned with water vapour and ozone in this region. He also carried out some of the first measurements showing the large amount of absorption of solar radiation by pollution. After four years at Farnborough he moved to London/Heathrow Airport, where he spent a couple of years as a forecaster on the upper-air bench, before in 1964 going to Met O 15, the then Atmospheric Physics Branch, at Bracknell.

For Dr Roach the year 1964 marked the beginning of his studies of atmospheric structure as it affects the operation and safety of aircraft. It was shortly after this that I first met Bill Roach while we were both studying severe thunderstorms in Oklahoma. His subsequent study of photographs from high-flying U2 aircraft provided the first direct evidence of storm tops penetrating 20 000 ft above the tropopause. He deduced that such penetrations implied updraughts as strong as $100 \mathrm{~m~s^{-1}}$ with extremely low temperatures within their upper parts. In recognition of the special importance of these studies for planning the operation of supersonic aircraft, Dr Roach was awarded the L.G. Groves Memorial Prize for Meteorology in 1967. Soon after his promotion to Principal Scientific Officer, in 1966 he moved to the Special Investigations Branch where he continued his work on aircraft hazards, studying clear air turbulence and giving advice on extremes to Concorde.

A new phase of work began in 1971 when Dr Roach moved back to Met O 15 which by then had become the Cloud Physics Branch. Apart from a short spell at the Meteorological Research Unit at Malvern in 1975, he remained in Met O 15 until 1977 carrying out a variety of studies, ranging from analysis of mesoscale wind fields in Project Scillonia to the effect of radiation on droplet growth. Using data gathered at the Meteorological Research Unit at Cardington he developed a better understanding of radiation fog. By explicitly modelling the details of the fog microphysics he and his colleagues demonstrated the importance of gravitational settling of fog droplets.

On promotion to Senior Principal Scientific Officer in 1977 Dr Roach became Assistant Director of the Special Investigations Branch. During the period to 1985 he was involved in a wide variety of work, including the forecasting of wind shear and severe storms, the automation of significant weather charts, the future use of aircraft wind and temperature data obtained via Data Link, and also the analysis of the spread and deposition of material from Australian nuclear tests. During the last three years, as Assistant Director at the Meteorological Research Flight (MRF), he has again had the opportunity to apply his years of experience in atmospheric radiation and cloud physics to the use of the Hercules aircraft. This has been an exciting period at MRF, with the modernization of the aircraft facilities and involvement in three major international experiments, HEXOS, FIRE and the Mesoscale Frontal Dynamics Project.

In retirement, Bill Roach intends to maintain his links with meteorology through his own personal research and through his membership of the Royal Meteorological Society and as its Treasurer. He and his wife Delia intend to remain for some time in the area and we wish them well over the coming years.

K.A. Browning

Restructuring of Branches within the Meteorological Office

Boundary Layer and Atmospheric Chemistry Branch (Met O 14)

The present role of Met O 14 in dealing with boundary layer research and the meteorological aspects of the release of material into the atmosphere will continue, but the Branch will take on additional responsibility for atmospheric chemistry. To this end the Atmospheric Chemistry Group from the old Cloud Physics Branch (Met O 15) has been transferred to Met O 14.

Meteorological Research Flight (Met O 15)

Research into radiation, cloud physics, and observational aspects of mesoscale and convective scale systems will be concentrated into a new Branch. Staff from the Cumulus and Stratocumulus Studies Group and the observational and technical groups within the old Met O 15 at Bracknell will join the Meteorological Research Flight (MRF) staff already at RAE Farnborough to strengthen the acquisition and analysis of data from the MRF aircraft. The Mesoscale and Convective Scale Research Group, although within the new Branch, is located at the University of Reading as part of the recently formed Joint Centre for Mesoscale Meteorology.

Remote Sensing Instrumentation Branch (Met O 19)

The Remote Sensing Instrumentation Branch will be formed from part of the old Satellite Meteorology Branch (Met O 19). It will work on advanced remote sensing instrument development, and deal with space-based, ground-based and airborne systems. The main activity of the Branch will be located at RAE Farnborough because of the need for easy access to the RAE/BNSC space test facility and the MRF aircraft. The Satellite Data Interpretation Techniques Group within the Hooke Institute at the University of Oxford will remain within this Branch for the time being.

Nowcasting and Satellite Applications Branch (Met O 24)

The new Branch will be concerned with the improved exploitation of remote sensing products in weather forecasting. It will consist of four groups dealing with:

(a) the manipulation and application of digital satellite data (work previously carried out in Met O 19),

(b) the interpretation of weather phenomena as aided by satellite and radar imagery (work previously done by the Satellite and Radar Studies Group in Met O 15),

(c) the development of FRONTIERS (work previously done by two groups in Met O 19), and

(d) the development and testing of very-short-range forecasting procedures and associated interactive work stations which will integrate remote sensing and numerical weather prediction products, and use expert system techniques as appropriate.

Forecasting Products Branch (Met O 8)

The Central Forecasting Branch (Met O 2) of the Meteorological Office had two main parts to it —the Central Forecasting Office (Met O 2a), concerned with producing operational analyses and forecasts, and Met O 2b, involved in the management and development of operational weather prediction facilities. In recognition of the wider support role which Met O 2b had acquired with the spread of automation throughout the Forecasting Services Directorate and with the provision of tailored model output directly to some commercial users, Met O 2b has been redesignated the Forecasting Products Branch and allocated the vacant Branch number Met O 8.

Fluid Dynamics Laboratory (Met O 21)

It is intended that a nucleus of the Fluid Dynamics Laboratory will be transferred to the Hooke Institute at the University of Oxford when arrangements with the University are finalized.

Review

Atmosphere, weather and climate, fifth edition, by R.G. Barry and R.J. Chorley. 156 mm × 234 mm, pp. xxii+460, *illus*. London, New York, Methuen, 1987. Price £30.00 (hardback), £10.95 (paperback).

The first edition (1968) of this book was judged as 'remarkably up to date' in an earlier *Meteorological Magazine* review. The fifth edition might be similarly described. It is aimed at geographers studying weather and climate in colleges, universities and sixth forms. Its aim is to impart an understanding of atmospheric processes, weather systems, climate (macro and micro), and climate change. As far as one who has neither taught nor studied geography can judge, the book is likely to meet these objectives. The authors are certainly eminently well qualified for the task, both being professors of geography.

The content is wide-ranging. The early chapters deal with atmospheric composition and structure, the effects of radiation, and the role of moisture. The central section explains atmospheric dynamics and the global circulation and goes on to discuss the weather and climate of temperate and tropical latitudes. Finally there is a chapter on small-scale climates — in plant canopies and cities — and one on climate variability and change. The scope is impressive and up to date. Numerical weather prediction and nowcasting are discussed as are climate models of various types. The El Niño Southern Oscillation phenomenon is described, so is the Sahel drought. The radiative effects of increasing CO_2 and other minor constituents of the atmosphere are discussed, and so are the effects of chlorofluorocarbons and oxides of nitrogen on atmospheric ozone. There is no reference to the relationship between sea surface temperature anomalies and Sahel rainfall nor any mention of the ozone hole. No doubt the sixth edition will rectify these omissions. The authors have also omitted any reference to 'nuclear winter'. Their restraint in not jumping on the bandwagon is commendable but a brief mention of the controversy should probably have been made. The section on observational data for weather forecasting is rather brief. More discussion of remote sensing would be worthwhile. The section on the tropics is a very good overview — one of the best modern introductions to tropical meteorology.

On the whole, the book is well written and readable. The text is clear, as are the diagrams, though one or two are a little dated. The book is well indexed and each chapter has plenty of references. Although the authors stated intention was to produce a 'non-technical' account they have included enough equations and explanation of physical processes to make the book useful to a wider audience than students of geography. Anyone teaching introductory courses in meteorology might well find the book sufficiently useful to buy it — I have already found it so, I keep my copy on my desk!

Professional meteorologists also, including forecasters, could usefully read it; they would gain a wider understanding of the topics covered outside their own specialism.

R. Kershaw

Books received

The listing of books under this heading does not preclude a review in the Meteorological Magazine at a later date.

Solar energy applications to buildings and solar radiation data, edited by T.C. Steemers (Dordrecht, Boston, London, Kluwer Academic Publishers, 1988. Dfl.125.00, US$69.00, £39.00) contains the proceedings of the second EC Contractors' Meeting held in Brussels in 1987, and is the fourth volume in the Solar Energy Development — Third Programme series. The reports presented give a full account of the current activities of the researchers and their co-operation in a European context.

Environmental meteorology, edited by K. Grefen and J. Löbel (Dordrecht, Boston, London, Kluwer Academic Publishers, 1988. Dfl.280.00, US$149.00, £84.00) contains the proceedings of an International Symposium held in Würzburg in 1987, which is intended to be the first in a series of symposia on the subject. Essentially, the many papers are concerned with the way meteorology acts as the link between emission and deposition of atmospheric pollutants.

Multiprocessing in meteorological models, edited by G.-R. Hoffmann and D.F. Snelling (Berlin, Heidelberg, New York, London, Paris, Tokyo, Springer-Verlag, 1988. DM 118.00) is a collection of papers presented at two workshops held at ECMWF. Trends to the migration to massive parallel systems in the near future are included.

Satellite and radar photographs — 28 July 1988

Fig. 1 shows a satellite image of a deepening depression which crossed the British Isles from the south-west giving 25 mm of rain in 24 hours over a wide swath across Ireland, North Wales and northern England. The well defined cloud bands had important repercussions on the rainfall distribution (Fig. 2) and the surface analysis.

A broad envelope of cloud associated with an old frontal zone extended from south-west to north-east across southern Britain and northern France. This was related to a gently ascending warm conveyor belt, W1 (see Fig. 3), whose northern limit was delineated by a band of cirrus, UU, marking the upper-level jet axis. Along the north coast of France, heavy rain occurred beneath a narrow band of warmer cloud tops, FF, lying along the surface front. Central and southern England were overlain by a layer of dry mid-level air beneath W1, and consequently the weather remained dry for much of the day.

The separate cloud canopy over Ireland and northern Britain originated from a secondary warm conveyor belt, W2, which emerged from beneath W1 and ascended rapidly over a warm frontal zone. This ascent, coupled with potential instability release within W2 (shown by the lumpy cloud structure over south-east Ireland), led to widespread heavy rain with rates widely exceeding 10 mm h^{-1}.

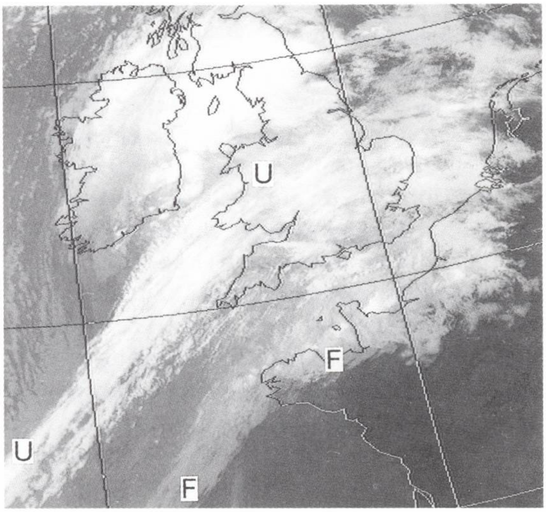

Figure 1. *Photograph by courtesy of University of Dundee*

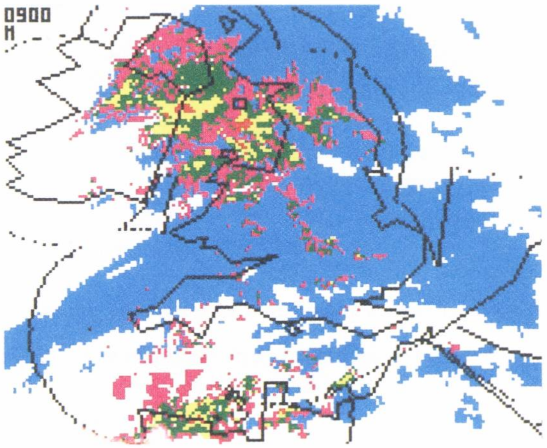

Figure 2.

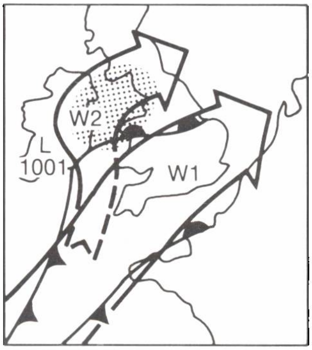

Figure 3.

Figure 1. NOAA-10 infra-red image for 0800 GMT.

Figure 2. Meteosat-derived infra-red cloud-top temperatures for 0900 GMT, light blue colder than −15 °C. Radar rainfall intensity (mm h^{-1}): pink <1, green 1–3, yellow 3–10, red >10. Coastlines, national boundaries and radar network boundaries are shown in black.

Figure 3. Location at 0900 GMT of the depression, surface fronts, and warm conveyor belts W1 and W2 referred to in the text. The area of heavy rain originating from W2 is stippled.

Meteorological Magazine

GUIDE TO AUTHORS

Content

Articles on all aspects of meteorology are welcomed, particularly those which describe the results of research in applied meteorology or the development of practical forecasting techniques.

Preparation and submission of articles

Articles for publication and all other communications for the Editor should be addressed to the Director-General, Meteorological Office, London Road, Bracknell, Berkshire RG12 2SZ and marked 'For *Meteorological Magazine*'.

Articles, which must be in English, should be typed, double-spaced with wide margins, on one side only of A4-size paper. Tables, references and figure captions should be typed separately.

Spelling should conform to the preferred spelling in the *Concise Oxford Dictionary*.

References should be made using the Harvard system (author, date) and full details should be given at the end of the text. If a document referred to is unpublished, details must be given of the library where it may be seen. Documents which are not available to enquirers must not be referred to.

Tables should be numbered using roman numerals and provided with headings. We consider vertical and horizontal rules to be unnecessary in a well-designed table; spaces should be used instead.

Mathematical notation should be written with extreme care. Particular care should be taken to differentiate between Greek letters and Roman letters for which they could be mistaken. Double subscripts and superscripts should be avoided, as they are difficult to typeset and difficult to read. Keep notation as simple as possible; this makes typesetting quicker and therefore cheaper, and reduces the possibility of error. Further guidance is given in BS1991: Part 1: 1976 and *Quantities, Units and Symbols* published by the Royal Society.

Illustrations

Diagrams must be supplied either drawn to professional standards or drawn clearly, preferably in ink. They should be about 1½ to 3 times the final printed size and should not contain any unnecessary or irrelevant details. Any symbols and lettering must be large enough to remain legible after reduction. Explanatory text should not appear on the diagram itself but in the caption. Captions should be typed on a separate sheet of paper and should, as far as possible, explain the meanings of the diagrams without the reader having to refer to the text.

Sharp monochrome photographs on glossy paper are preferred: colour prints are acceptable but the use of colour within the magazine is at the Editor's discretion. In either case contrast should be sufficient to ensure satisfactory reproduction.

Units

SI units, or units approved by WMO, should be used.

Copyright

Authors wishing to retain copyright for themselves or for their sponsors should inform the Editor when they submit contributions which will otherwise become UK Crown copyright by right of first publication.

It is the responsibility of authors to obtain clearance for any copyright material they wish to use before submitting it for publication.

Free copies

Three free copies of the magazine are provided for authors of articles published in it. Separate offprints for each article are not provided.

Meteorological Magazine

October 1988

Vol. 117
No. 1395

CONTENTS

Contributions: It is requested that all communications to the Editor and books for review be addressed to the Director-General, Meteorological Office, London Road, Bracknell, Berkshire RG12 2SZ, and marked 'For *Meteorological Magazine*'. Contributors are asked to comply with the guidelines given in the *Guide to authors* which appears on the inside back cover. The responsibility for facts and opinions expressed in the signed articles and letters published in *Meteorological Magazine* rests with their respective authors. Authors wishing to retain copyright for themselves or for their sponsors should inform the Editor when submitting contributions which will otherwise become UK Crown copyright by right of first publication.

Subscriptions: Annual subscription £27.00 including postage; individual copies £2.30 including postage. Applications for postal subscriptions should be made to HMSO, PO Box 276, London SW8 5DT; subscription enquiries 01–211 8667.

Back numbers: Full-size reprints of Vols 1–75 (1866–1940) are available from Johnson Reprint Co. Ltd, 24–28 Oval Road, London NW1 7DX. Complete volumes of *Meteorological Magazine* commencing with volume 54 are available on microfilm from University Microfilms International, 18 Bedford Row, London WC1R 4EJ. Information on microfiche issues is available from Kraus Microfiche, Rte 100, Milwood, NY 10546, USA.

ISBN 0 11 728089 5

ISSN 0026–1149

Printed in the United Kingdom for Her Majesty's Stationery Office
Dd 0240021 C13 9/88 3936 12521